Technical Report

TR-04-05

The effect of discontinuities on the corrosion behaviour of copper canisters

F King
Integrity Corrosion Consulting Ltd,
Calgary, Alberta, Canada

March 2004

Svensk Kärnbränslehantering AB
Swedish Nuclear Fuel
and Waste Management Co
Box 5864
SE-102 40 Stockholm Sweden
Tel 08-459 84 00
+46 8 459 84 00
Fax 08-661 57 19
+46 8 661 57 19

The effect of discontinuities on the corrosion behaviour of copper canisters

F King
Integrity Corrosion Consulting Ltd,
Calgary, Alberta, Canada

March 2004

Keywords: Copper, Corrosion, Canister, Localised corrosion, Pitting, Stress corrosion cracking, Initiation, Propagation, Geologic repository, Spent nuclear fuel.

Abstract

Discontinuities may remain in the weld region of copper canisters following the final closure welding and inspection procedures. Although the shell of the copper canister is expected to exhibit excellent corrosion properties in the repository environment, the question remains what impact these discontinuities might have on the long-term performance and service life of the canister. A review of the relevant corrosion literature has been carried out and an expert opinion of the impact of these discontinuities on the canister lifetime has been developed.

Since the amount of oxidant in the repository is limited and the maximum wall penetration is expected to be < 2 mm, discontinuities will only be significant if they impact the localised corrosion or stress corrosion cracking (SCC) behaviour of the canister.

Not all of the discontinuities will impact the corrosion behaviour of the canister. Only surface-breaking discontinuities and those discontinuities within 2 mm of the surface will affect the corrosion behaviour. Defects located further away from the finished surface will have no impact.

The relevant literature on the initiation and propagation of localised corrosion and SCC has been reviewed. Initiation of localised corrosion occurs at the microscopic scale at grain boundaries, and will not be affected by the presence of macroscopic discontinuities. The localised breakdown of a passive $Cu_2O/Cu(OH)_2$ film at a critical electrochemical potential determines where and when pits initiate, not the presence of pit-shaped surface discontinuities.

The factors controlling pit growth and death are well understood. There is evidence for a maximum pit radius for copper in chloride solutions, above which the small anodic: cathodic surface area ratio required for the formation of deep pits cannot be sustained. This maximum pit radius is of the order of 0.1–0.5 mm. Surface discontinuities larger than this size are unlikely to propagate as pits, and pits generated from smaller discontinuities will die once they reach this maximum size. Death of propagating pits will be compounded by the decrease in oxygen flux to the canister as the repository environment becomes anoxic.

Surface discontinuities could impact the SCC behaviour either through their effect on the local environment or via stress concentration or intensification. There is no evidence that surface discontinuities will affect the initiation of SCC by ennoblement of the corrosion potential or the formation of locally aggressive conditions.

Stress concentration at pits could lead to crack initiation under some circumstances, but the stress intensity factor for the resultant cracks, or for pre-existing crack-like discontinuities, will be smaller than the minimum threshold stress intensity factor (K_{ISCC}) for copper reported in the literature. Therefore, any cracks that do initiate will tend to become dormant.

In summary, there is no evidence that weld discontinuities will adversely affect the localised corrosion or SCC behaviour of copper canisters. The predicted service life of the canisters is not affected by the presence of such features.

Content

1 Introduction

The proposed method for the disposal of spent fuel in Sweden involves the encapsulation of the waste in canisters comprising an inner cast iron insert and an outer oxygen-free copper shell (Figure 1-1). These canisters would be emplaced in an engineered repository located at a depth of 500–700 m in the granitic rock of the Fenno-Scandian Shield /SKB, 1983/. For the environmental conditions expected to prevail in the repository, the predicted service lifetime of the canister exceeds one million years /King et al, 2001/. The integrity of the canister is primarily a result of the excellent corrosion properties of copper in the repository environment.

After loading, the canister will be sealed with a final closure weld. Two welding procedures are being investigated, electron beam and friction stir welding /Werme, 2000/. Regardless of the welding procedure used, the final closure weld will be inspected. Both the final closure weld and weld inspection have to be performed remotely. The two inspection techniques under investigation are X-ray radiography and ultrasonic inspection /Werme, 2000/.

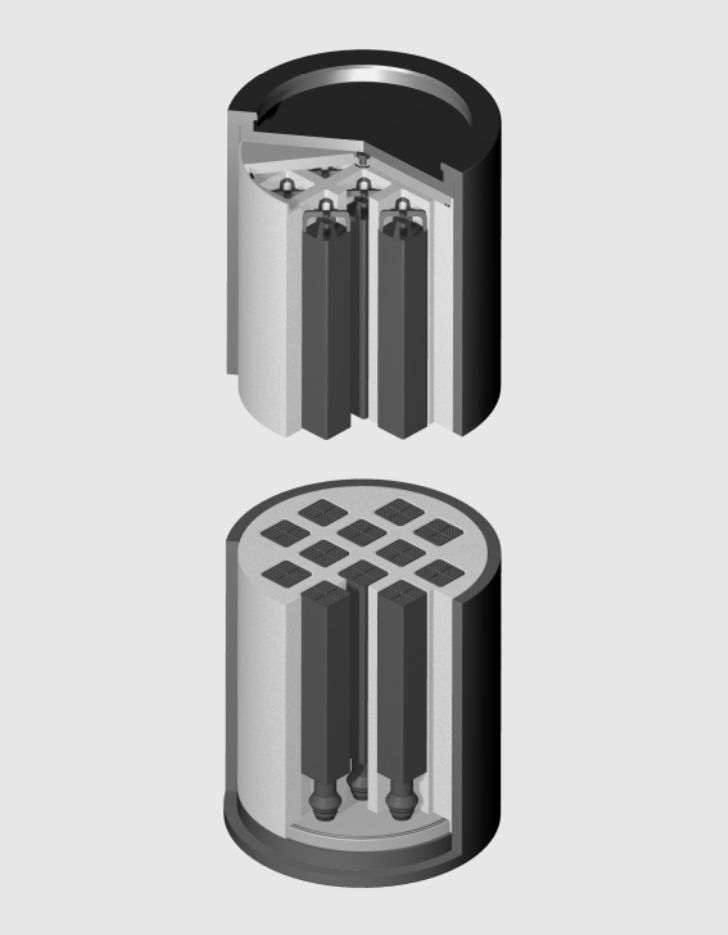

Figure 1-1. *Overall view of a spent BWR fuel disposal canister illustrating the cast iron insert and outer copper shell corrosion barrier.*

Inevitably, some manufacturing flaws (discontinuities) will remain in the canister after welding and inspection. No inspection procedure can be 100% reliable and it may be impractical to remove or repair all discontinuities associated with the final closure weld. The number, shape, size, and location of such flaws is not currently known, but the question arises of what effect these remaining discontinuities will have on the subsequent corrosion behaviour of the canister? Since the amount of available oxidant in the repository is insufficient to cause failure of the canister by general corrosion /King et al, 2001; Werme et al, 1992/, the greatest concern is the effect of surface-breaking and near-surface defects on the localised corrosion and stress corrosion cracking (SCC) behaviour of the canister.

This report includes a review of the localised corrosion and SCC of copper and presents an analysis of the effect of discontinuities on the service life of the canister. Some background information on the likely size, shape, and distribution of discontinuities is presented in Section 2, followed by a review of the mechanisms of the initiation and propagation of localised corrosion and SCC of copper. The effect of surface and near-surface discontinuities on the corrosion of the canister is discussed in Section 4, along with an assessment of their effect on the canister lifetime.

2 Background

The majority of the discontinuities in the canister shell will be associated with the final closure weld. Figure 2-1 shows the proposed weld configuration prior to welding. The weld will be performed horizontally, with the fronting bar on the right-hand side of the lid preventing the weld pool from poring out of the weld. The fronting bar will be machined flush with the side of the canister wall after welding. To achieve adequate fusion, the weld must penetrate approximately 65 mm from the outer surface of the canister.

Figure 2-2 shows a number of discontinuities that have been found during preliminary electron beam welding trials at the SKB Canister Laboratory in Oskarshamm. The discontinuities exhibit a variety of shapes and sizes. Those in Figures 2-2a and 2-2b vary from ~ 4 to 20 mm in length. The pores are generally elongated in shape and orientated with their long axis aligned radially. Some are surface breaking, as illustrated in Figures 2-2c and 2-2e, whereas others are sub-surface (Figures 2-2d and 2-2f). The discontinuity in Figure 2-2e has the characteristics of an under-cut pit, with a relatively narrow opening to the environment and a wide radius below the surface. The discontinuity in Figure 2-2f shows similar characteristics, along with a tapered acute tip at the deepest part of the pore.

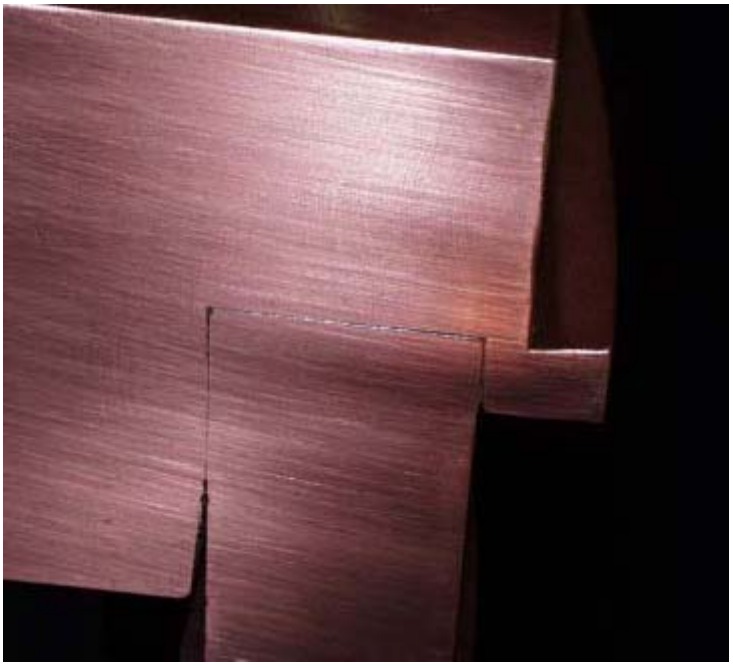

Figure 2-1. *Proposed closure weld configuration prior to welding.*

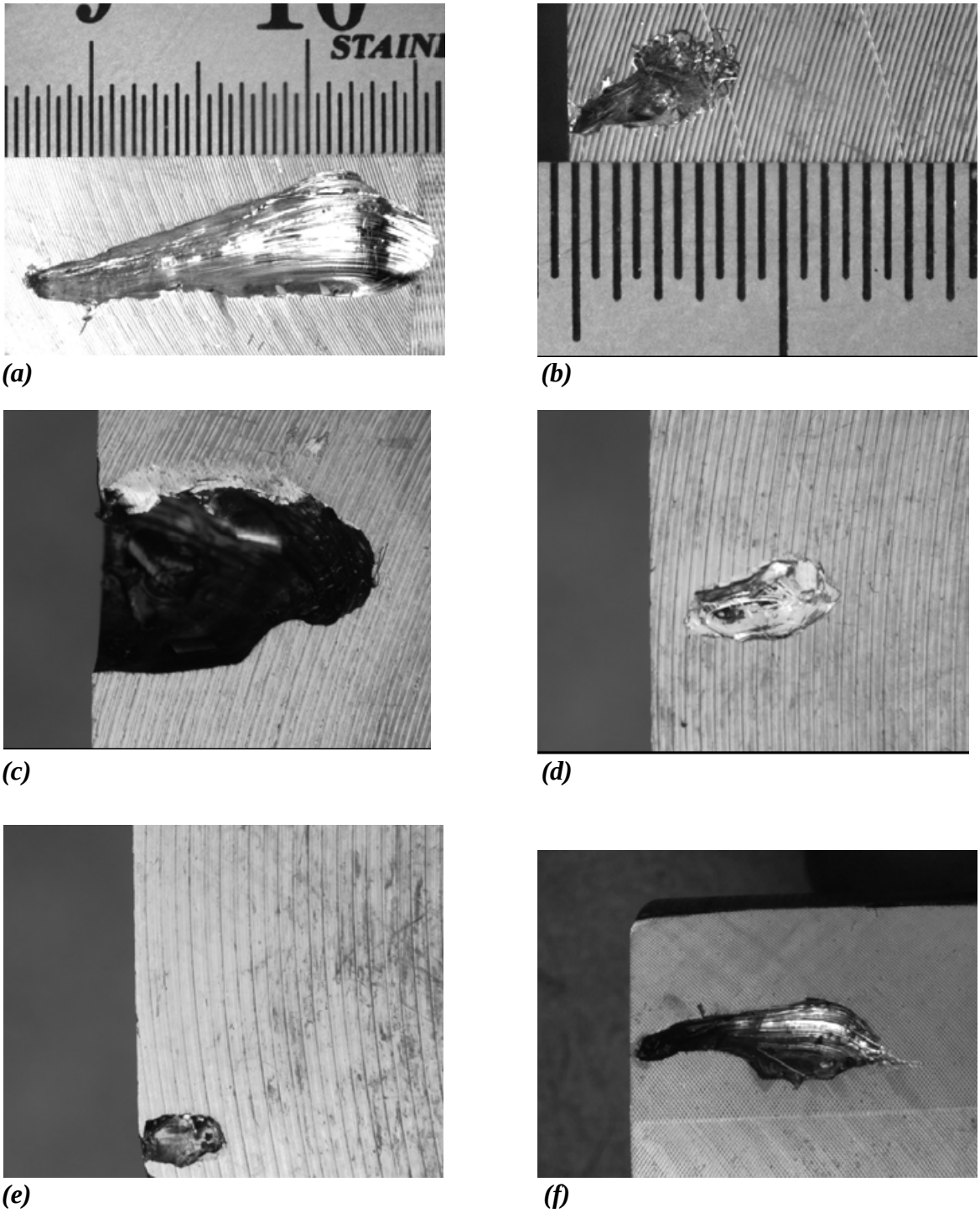

Figure 2-2. *Examples of discontinuities in welds from preliminary trials at the SKB Canister Laboratory.*

In addition to the surface-breaking and near-surface discontinuities shown in Figure 2-2, there are pores found along the entire length of the weld. Figure 2-3 shows the results from X-ray radiography of a test weld from the Canister Laboratory. Whilst those discontinuities deep into the weld may be said to affect the overall weld quality, they pose no problem from the point-of-view of the lifetime of the canister. Because of the lack of oxidant in the repository, the maximum wall penetration due to corrosion is estimated to be < 2 mm, even for the most conservative of assumptions /King et al, 2001/. Therefore, the porosity at the weld root (location 1 in Figure 2-3) would not impact the service life of the canister. On the other hand, the discontinuities at locations 2 and 3 might be significant, depending upon how close they are to the surface following machining of the fronting bar and canister wall and if they can serve as initiation points for localised corrosion.

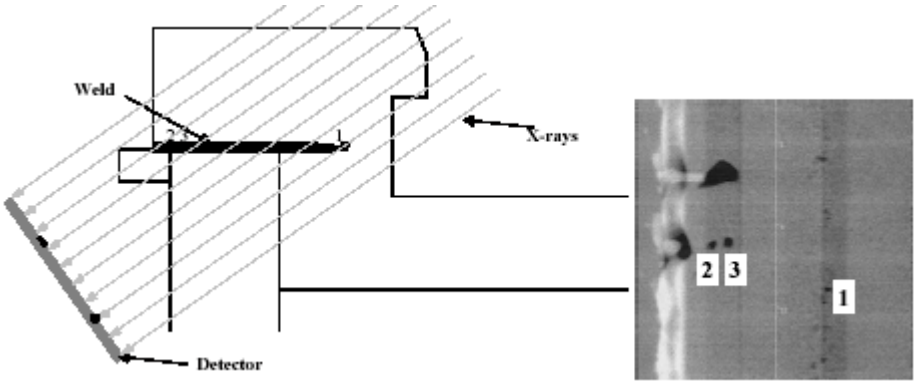

Figure 2-3. *Location of discontinuities along the length of the weld as determined by X-ray radiography.*

3 Mechanisms of localised corrosion and SCC of copper

3.1 Localised corrosion

Localised corrosion, i.e. the preferential dissolution of the surface in a discrete localised region, can be broadly divided into two stages: initiation and propagation. The literature relevant to the localised corrosion of copper canisters has been reviewed elsewhere /King et al, 2001/. Here, evidence is presented to address the questions:

Can the presence of surface defects increase the probability of the initiation of localised corrosion?

Does the presence of surface defects increase the rate, or prolong the duration, of localised penetration?

In order to answer these questions, it is useful to consider the mechanism of the pitting of copper in terms of pit initiation, growth, and pit depth. By understanding the factors that contribute to each of these stages of localised corrosion it should be possible to answer the questions of whether pre-existing discontinuities pre-dispose the canister surface to the initiation and/or propagation of pits.

3.1.1 Initiation

Various mechanisms have been proposed for the initiation of pitting of copper, but all share the same basic requirements. Pitting, either in fresh potable water or in more-concentrated chloride solutions such as those to which the canister may be exposed, requires (i) the presence of a passive Cu_2O and/or $Cu(OH)_2$ film, (ii) Cl^- ions, and (iii) a surface potential more positive than a critical potential for pit initiation (usually referred to as the pitting or breakdown potential (E_B) /King et al, 2001/).

Figure 3-1 shows a comparison between the corrosion potential (E_{CORR}) and E_B as a function of pH in 0.5 mol·dm^{-3} Cl^- solution /King, 2002/. Also shown on the figure are the equilibrium lines for the formation of Cu_2O and $Cu_2O/Cu(OH)_2$ predicted from thermodynamic data. There is a clear association between the initiation of pitting and the presence of a surface film, although the data in Figure 3-1 suggest the film in question may be a $Cu_2O/Cu(OH)_2$ rather than Cu_2O. The variation of E_B with [Cl^-], temperature, and the presence of bicarbonate ions has been discussed elsewhere /King, 2002; King et al, 2001/.

The available evidence indicates that pits tend to initiate at grain boundaries or at triple points /Al-Kharafi et al, 1989; de Chialvo et al, 1985; Shalaby et al, 1989/. These locations represent sites at which the protective Cu_2O film is most likely to break down, because the film will tend to be thicker, more porous and more defected /Al-Kharafi et al, 1989/. Others suggest that pit initiation occurs randomly over the surface and, as support, present evidence that the surface pit distribution follows a Poisson distribution (Figure 3-2) /Laz et al, 1992/. The difference between these two studies probably lies in the different definitions of an initiated pit. /Laz et al, 1992/ observed small (~ 4 μm diameter) crystallographic etch pits, whereas /Al-Kharafi et al, 1989/ were more concerned with initiation events that led to fully propagating pits. Regardless, it is apparent that pit initiation occurs at the microscopic level on a scale of the order of the size of a single grain or smaller.

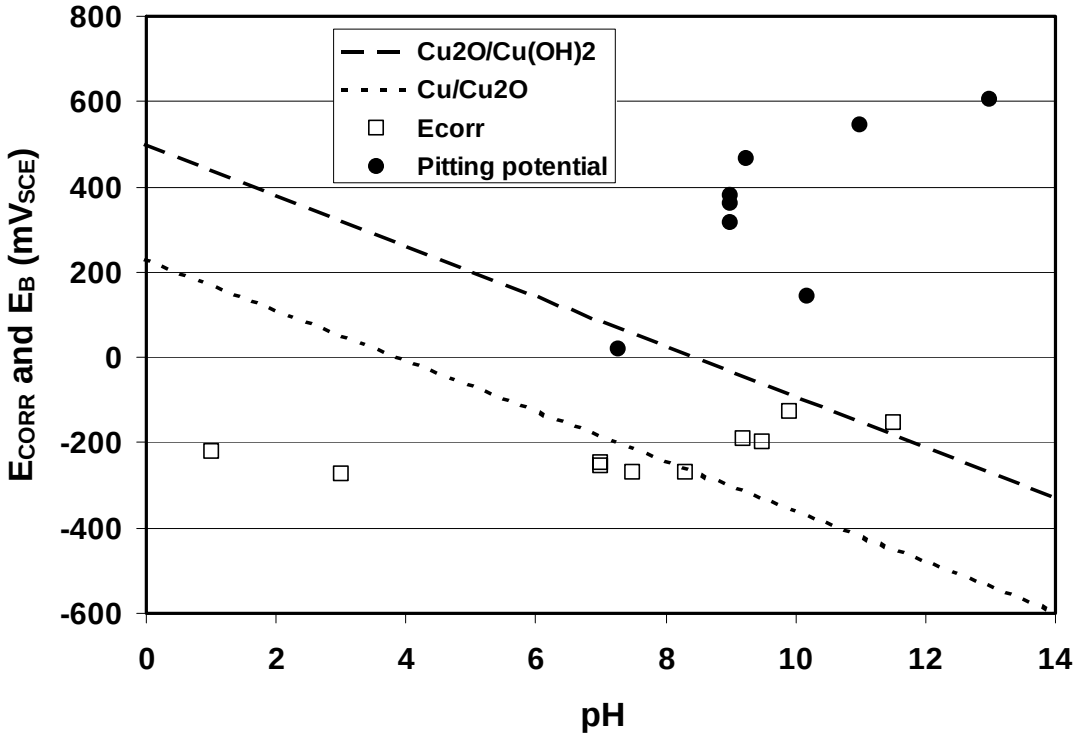

Figure 3-1. *Dependence of the breakdown potential for pitting (E_B) and the corrosion potential (E_{CORR}) on pH in 0.5 mol·dm^{-3} chloride solution /King, 2002/.*

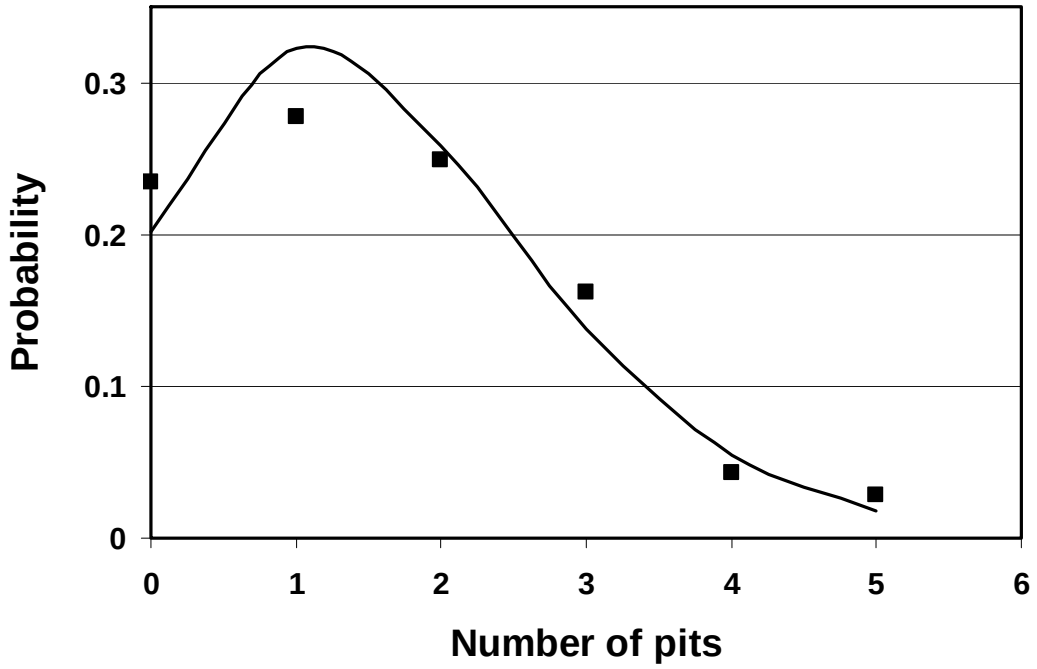

Figure 3-2. *Probability of finding a given number of pits within a radius of approximately 10 µm of another pit /Laz et al, 1992/.*

Figures 3-3 to 3-5 show three mechanisms for the initiation (and propagation) of pits on copper. All three mechanisms assume pit initiation occurs at grain boundaries, due either to the rupture of the film at this location or to the preferential dissolution as $CuCl_2^-$ through the passive film. In Lucey's mechanism (Figure 3-3), a CuCl pocket is formed under a Cu_2O layer following Cl^- diffusion through the film or the hydrolysis of $CuCl_2^-$ dissolving locally at the grain boundary. Continued dissolution of this pocket through the Cu_2O film eventually leads to the familiar cap-covered pit characteristic of Lucey's mechanism (see below). /de Chialvo et al, 1985/ propose that the CuCl pocket is formed under a duplex Cu_2O/CuO or $Cu_2O/Cu(OH)_2$ film, which seems more consistent with the observed correlation between the breakdown potential and the equilibrium potential for this latter process (Figure 3-1). /King and Kolar's, 2000/ mechanism was developed more to address

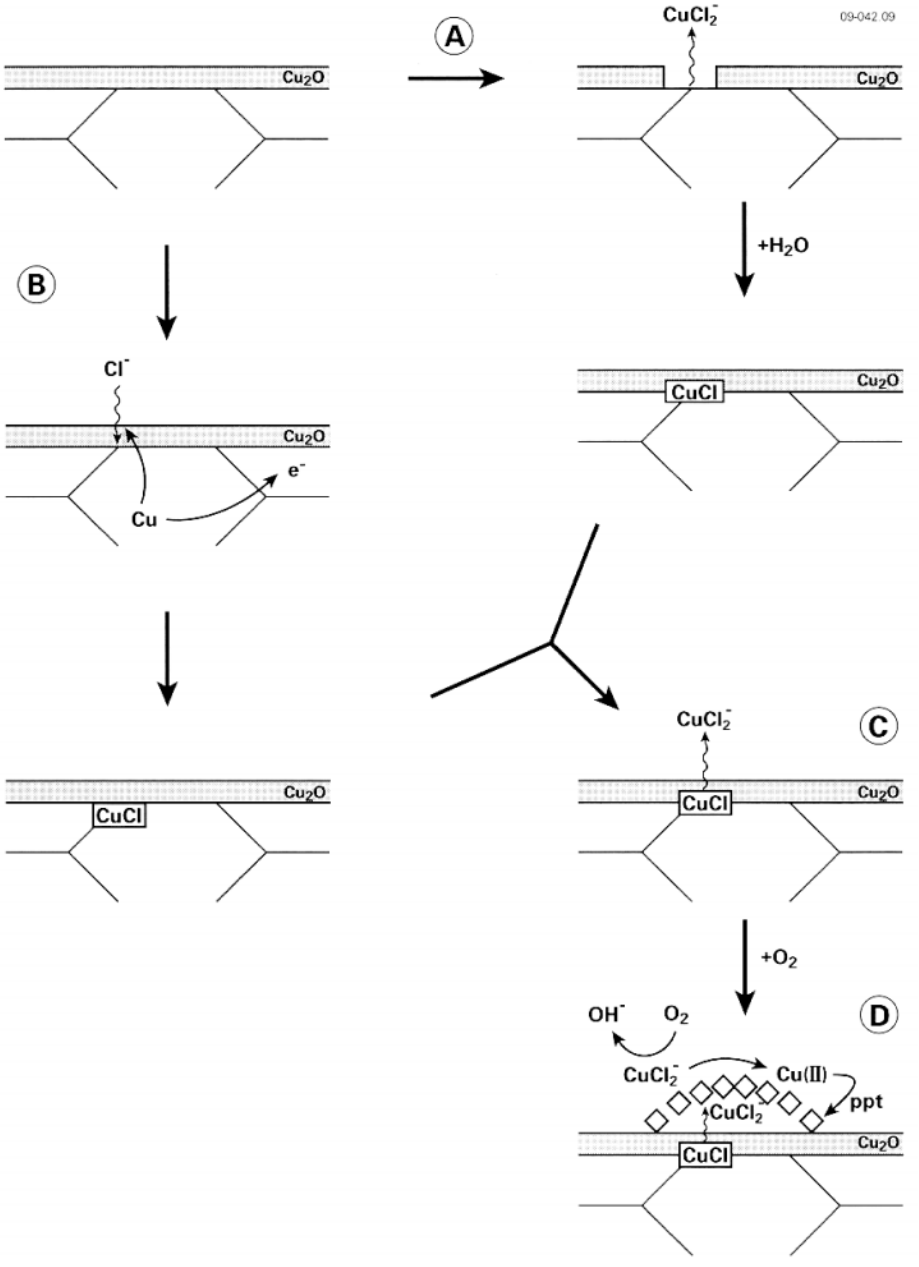

Figure 3-3. *Mechanism for the initiation of Type I pitting of copper due to the formation of a CuCl pocket, after /Lucey, 1967/.*

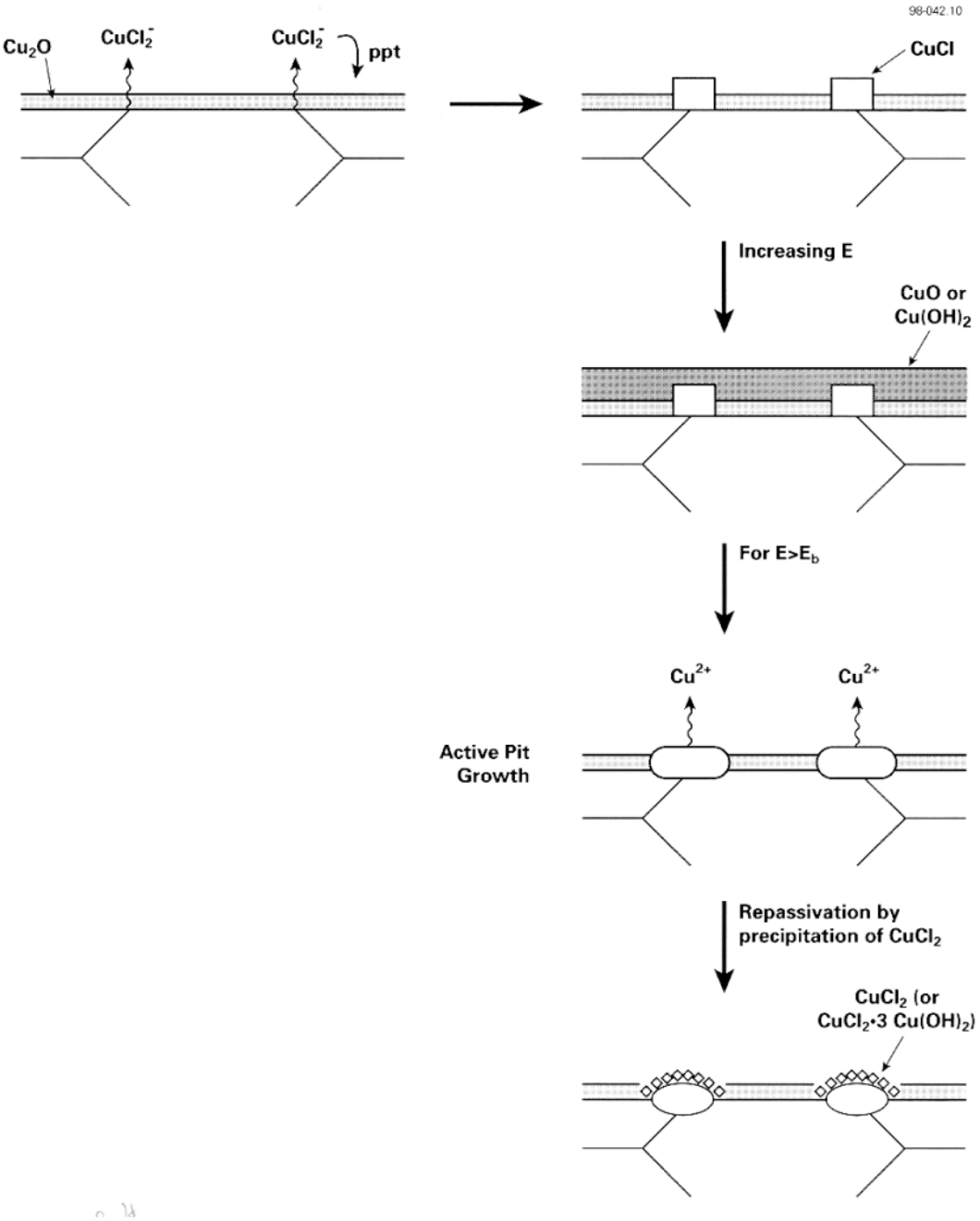

Figure 3-4. *Initiation and propagation mechanisms proposed by /de Chialvo et al, 1985/ for the pitting of copper in chloride solutions.*

the propagation of localised corrosion than its initiation, but also includes initiation at grain boundaries via localised dissolution or film breakdown at these locations.

The significant feature of all these initiation mechanisms is that the process occurs on a microscopic scale. Localised defects in the passive film and the presence of Cl^- are sufficient to drive the formation of a pit. Macroscopic defects, such as those that might remain after the final closure weld, are not required to initiate localised corrosion of the canister.

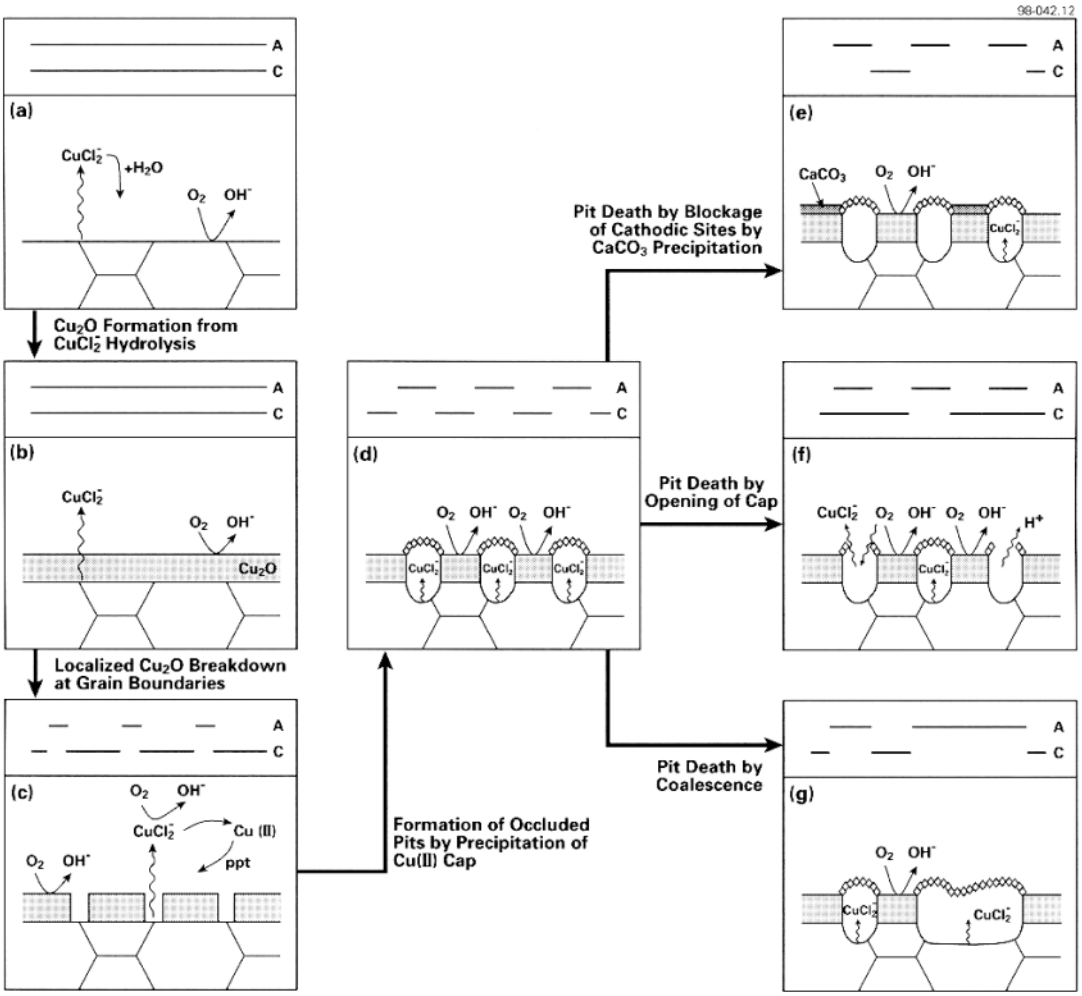

Figure 3-5. *Proposed mechanism for the under-deposit corrosion of copper canisters under conditions simulating those in a deep geologic repository /King and Kolar, 2000/.*

3.1.2 Propagation

There are a number of pre-requisites for pit propagation on copper surfaces, namely:

1. a supply of oxidant (generally, either O_2 or cupric ions Cu(II)),
2. sustained separation of the anodic and cathodic reactions by a precipitated cap of corrosion products, and
3. a small anode:cathode surface area ratio (although anodic and cathodic surface areas are of similar size in the Lucey mechanism).

If all of these factors are not present, then the pit will inevitably stifle and die.

Various mechanisms have been proposed for the propagation of pits on copper /King et al, 2001/, a number of which are reviewed here. The most famous mechanism is that proposed by /Lucey, 1967/ to explain the Type I pitting of copper water pipes in potable water. Figure 3-6 shows a cross-section through a pit and illustrates the reactions inherent in Lucey's mechanism. Anodic dissolution of copper in the base of the pit is supported by the cathodic reduction of Cu(II) in the upper half of the pit. The two electrochemical processes are separated by a porous, electrically conducting Cu_2O membrane. To maintain pit growth,

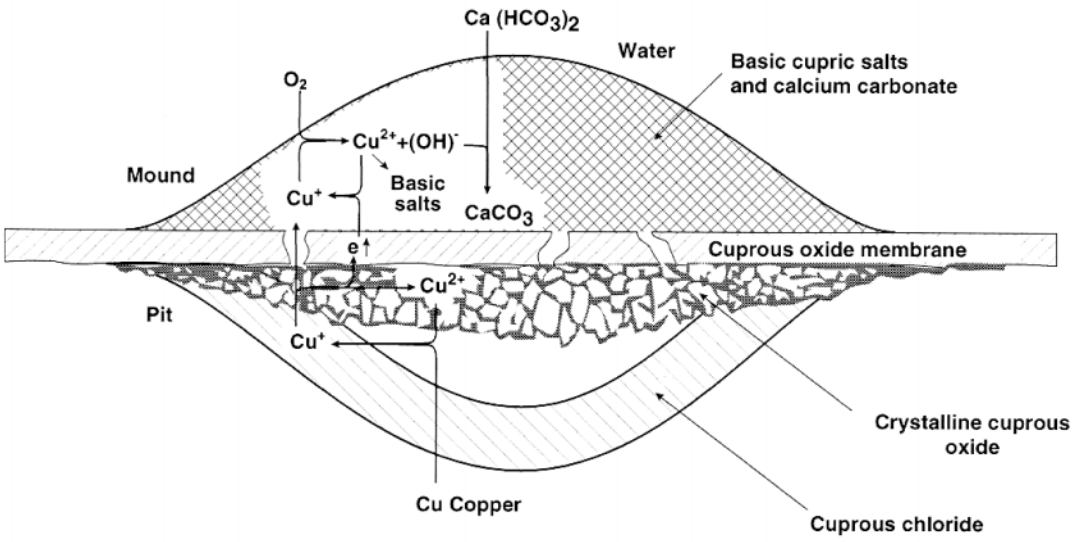

Figure 3-6. *Cross-section through a Type I pit on copper illustrating the electrochemical, chemical, and mass-transport processes involved in pit propagation /Lucey, 1967/.*

a continuous supply of O_2 is required to generate Cu(II) in the upper half of the membrane cell.The anode is only maintained as long as the cap of corrosion products is present, thus preventing the diffusive and advective loss of oxidant from the occluded region. The unusual co-location of both anodic and cathodic reactions with approximately equal surface area within the occluded region accounts for the hemi-spherical shape commonly observed for this type of pitting. Others have suggested that the cathode is more conventionally located on the exposed copper surface outside of the occluded region under the cap of corrosion products /Campbell, 1974/. Under chemical conditions associated with Type I pitting, /Sosa et al, 1999/ have determined that as much as 90% of the total cathodic charge is associated with processes occurring outside the pit, raising the possibility of lower aspect ratio (i.e. half-width/depth) pits.

In the mechanism proposed by /de Chialvo et al, 1985/ for the pitting of copper in chloride solutions (Figure 3-4), pit propagation occurs via the dissolution of copper as Cu(II) species. This requires that the potential is sufficiently positive ($E > E_B$) that Cu(II) is formed directly by dissolution, and not as a by-product of the homogeneous oxidation of Cu(I) by O_2. Given that Cu(I) is stabilised in Cl^- solutions via complex ion formation (i.e. as $CuCl_2^-$, $CuCl_3^{2-}$, etc. species), the potential must exceed a value of ~ 0 V_{SCE} /King and Kolar, 2000/. Such a potential can only be achieved in the presence of O_2 and/or Cu(II).

The mechanism proposed by /King and Kolar, 2000/ was developed to explain the under-deposit corrosion observed on copper surfaces exposed to compacted bentonite saturated with a saline ground water solution. Following removal of the precipitated corrosion products, the underlying copper surface was found to be roughened (Figure 3-7). Although the surface is roughened, the entire surface has been corroded (note the position of the original surface of the coupon noted on the figure), suggesting the non-permanent separation of anodic and cathodic sites. The surface was covered by the same corrosion products ($CaCO_3$, $CuCl_2 \cdot 3Cu(OH)_2$) as observed for the pitting of copper in chloride environments.

/King and Kolar, 2000/ proposed a mechanism to explain these observations that accounted for both pit propagation and death (Figure 3-5). Propagation is characterised by an anodic:cathodic surface area ratio < 1 and pit death by a value > 1. Propagation was

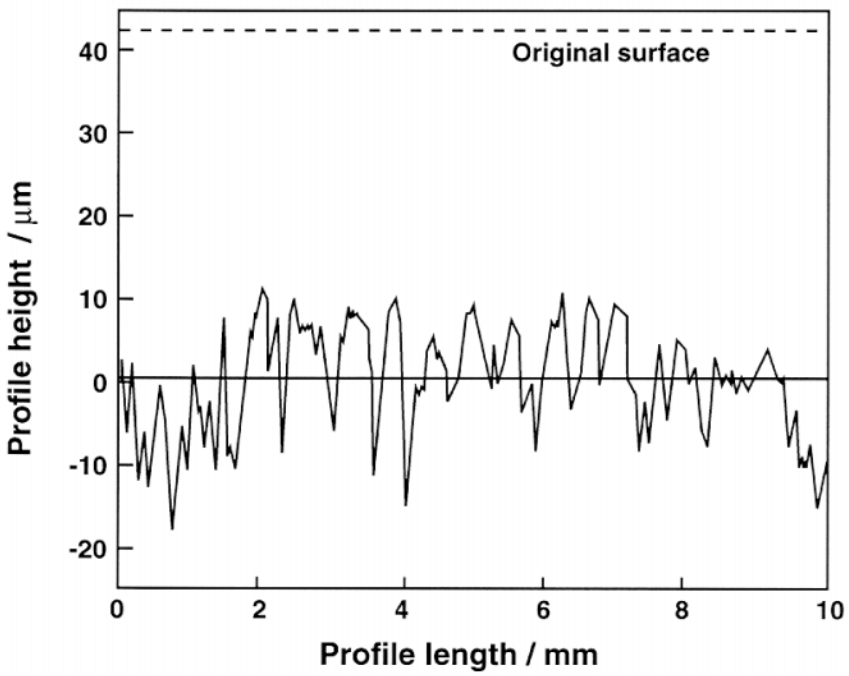

Figure 3-7. *Surface profile of copper specimen exposed to compacted bentonite:sand buffer material saturated with aerated saline ground water at 50°C for 733 days /King and Kolar, 2000/.*

considered to occur in an occluded region formed by the precipitation of $CaCO_3$ and/or $CuCl_2 \cdot 3Cu(OH)_2$

(Figure 3-5d). Continued propagation is contingent on the maintenance of the occluded region and a supply of oxidant (O_2 or, possibly, Cu(II)). Three processes were considered that could lead to pit death: (i) blockage of cathodic sites by the precipitation of $CaCO_3$, (ii) opening of the cap of corrosion products, allowing diffusive mixing of the occluded and bulk environments, and (iii) coalescence of pits, thus increasing the anodic:cathodic surface area ratio (Figures 3-5e to g, respectively). The respective locations of the anodic (A) and cathodic (C) processes are illustrated in the upper pane of each figure.

The factors that might lead to pit death by each of these routes were not discussed by /King and Kolar, 2000/, but the increasing radius of a propagating pit would tend to lead to pit death by either the pit-opening or pit-coalescence routes. The larger the pit, the more likely the cap of corrosion products is to become defected by internal stresses. In addition, larger pits are more likely to coalesce with other neighbouring pits.

If increasing pit diameter promotes death by the pit-opening or pit-coalescence mechanisms, then an estimate of the maximum pit diameter can be obtained from the profile in Figure 3-7. The profile exhibits approximately 37 peaks, representing 36 “pits” with a mean diameter of 0.28 mm. Another estimate of the maximum pit diameter can be obtained from the data of /Mankowski et al, 1997/, who characterised pits formed on copper in chloride and sulphate environments. Figure 3-8 shows a series of coalesced pits formed on copper in 0.1 $mol \cdot dm^{-3}$ Cl^- solution. The average diameter of the individual pits is of the order of a few tenths of a mm, the same as that inferred from Figure 3-7.

There is evidence, therefore, for a maximum pit diameter on copper exposed to Cl^- solutions. Pits with a diameter greater than a few tenths of a mm tend to coalesce and will inevitably die as the suddenly increased anodic:cathodic surface area ratio is insufficient to sustain the acidified anodic electrolyte inside the occluded cell. Pit opening would also lead

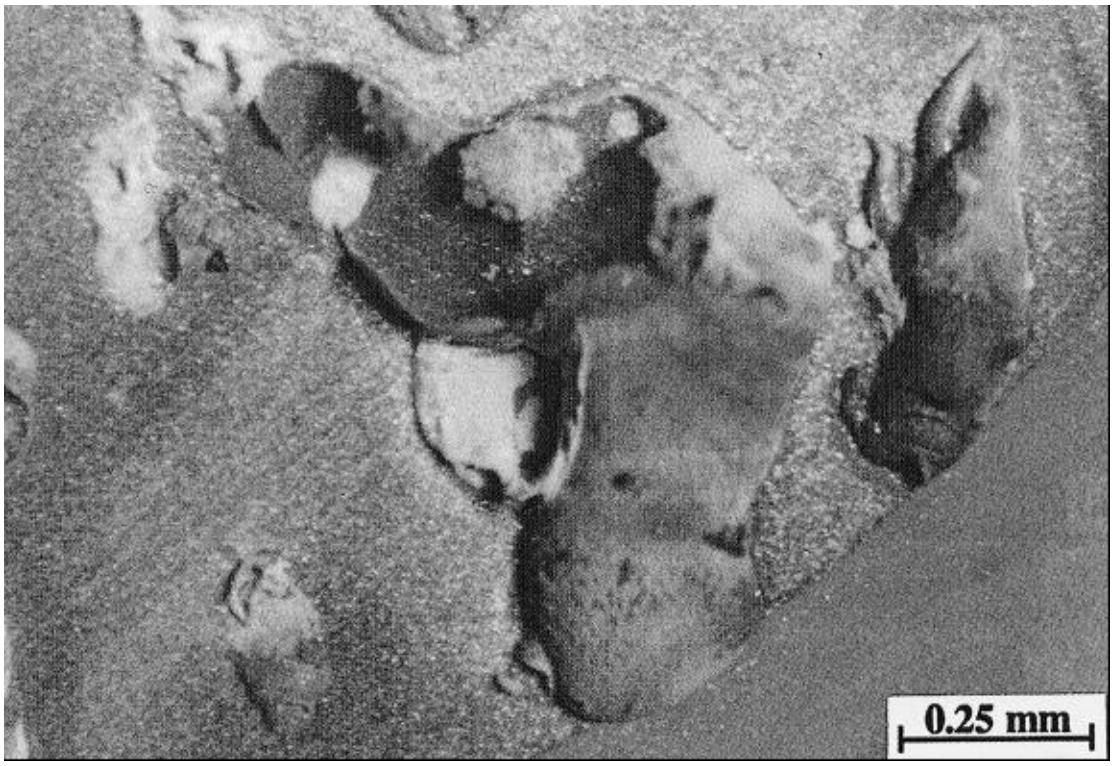

Figure 3-8. *Photograph of overlapping pits on copper exposed to 0.1 mol·dm^{-3} chloride solution /Mankowski et al, 1997/.*

to an increase in anodic:cathodic surface area ratio and pit death. However, although fracturing of the corrosion product is more likely to occur as the pit diameter increases, there is no direct experimental evidence that this mechanism contributes to the non-permanent separation of anodic and cathodic sites evident from the profile in Figure 3-7.

Additional experimental evidence that there is a maximum diameter for the formation of a stable occluded pit comes from the results of a limited series of tests reported by /Ryan et al, 1994/. Various types of copper coupon were exposed to a synthetic ground water/bentonite slurry at a temperature of 100°C in the presence of a γ-radiation field (absorbed dose rate 4.5 Gy/hr), with a maximum exposure period of 4.0 yr. The ground water was initially aerated and had a Cl^- concentration of 0.97 mol·dm^{-3}. Among these samples were two so-called artificially pitted coupons (Figure 3-9). The samples (approximately 2.5 cm long x 1.25 cm wide x 0.63 cm deep) contained two rows of drilled holes (~ 0.5 mm diameter x 2-4 mm deep) to simulate pre-existing pits. The aim of the test was to determine whether these "pits" would propagate under simulated repository conditions.

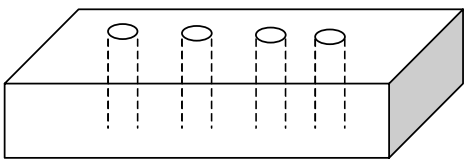

Figure 3-9. *Schematic of the artificially pitted copper sample exposed to simulated repository conditions by /Ryan et al, 1994/. For clarity, only a single row of "pits' is shown. See text for details regarding the sample and exposure conditions.*

At the end of the exposure period, the samples were examined for evidence of preferential localised corrosion in and surrounding the artificial pits. No such localised attack was observed, the drilled holes retaining the sharp edges of the original machining. No cap of corrosion products or precipitated $CaCO_3$ formed over the pits, which instead became filled with clay particles from the ground water/bentonite slurry used in the tests.

Another experimental technique used to determine the propensity for pit propagation is the measurement of the re-passivation potential (E_{RP}) of propagating pits (Figure 3-10). Pits are generally initiated electrochemically by scanning the potential in the positive (anodic) direction until the potential exceeds E_B. Reversing the direction of the potential scan typically results in higher currents during the reverse scan due to propagation of the newly initiated pits. Eventually, however, the pits re-passivate as the potential is scanned to more-negative potentials and the driving force for dissolution diminishes. In effect, such tests represent the initiation, propagation, and pit death processes considered by /King and Kolar, 2000/ (Figure 3-5).

Table 3-1 shows data for the breakdown, re-passivation and corrosion potentials of oxygen-free copper in various synthetic ground water solutions /Sridhar and Cragnolino, 1993/. Relatively few instances of pitting were reported by these authors and in many cases the values of E_{RP} and E_B are identical.

The results in Table 3-1 support the concept that propagating pits on copper re-passivate relatively easily. The limited data presented by /Sridhar and Cragnolino, 1993/ on the nature of the pitting that was observed suggests that, although initiation as micro-pits occurs readily, the maximum pit diameter is of the order of 0.1 mm. The largest pits appeared to be formed by the coalescence of smaller pits, as illustrated in Figure 3-5 g. The re-passivation of growing pits in the laboratory by scanning the potential to more-cathodic potentials is analogous to re-passivation of pits on a copper canister due to a decrease in the amount of available oxidant. The function of both the potentiostat in the laboratory and the oxidant in a naturally corroding system is to sustain copper dissolution in the occluded cell at a sufficient rate to prevent re-passivation.

In summary, the continued propagation of pits requires (i) a sufficient source of oxidant (O_2 or Cu(II)), (ii) a persistent occluded geometry created by a cap of corrosion products, and (iii) a small anodic:cathodic surface area ratio (for the formation of low aspect ratio pits). In

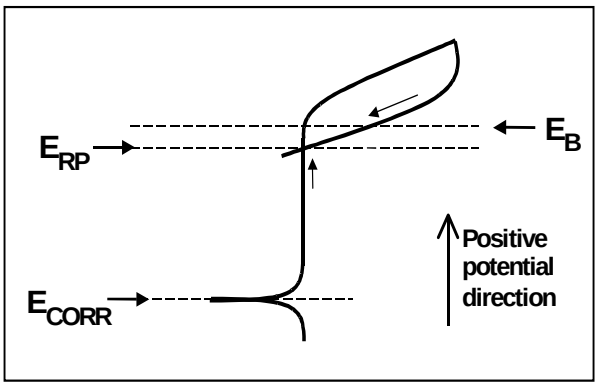

Figure 3-10. *Schematic illustrating the measurement of the breakdown (E_B) and re-passivation (E_{RP}) potentials for localised corrosion of a passive material in cyclic polarisation experiments. The corrosion potential (E_{CORR}) is shown schematically and is best determined in separate experiments in which the sample is not polarised.*

Table 3-1. Comparison of corrosion, breakdown, and re-passivation potentials in various environments /Sridhar and Cragnolino, 1993/. The tests in which pits were visually seen on the coupon surface are highlighted in bold font

$[Cl^-]$ (µg/g)	$[HCO_3^-]$ (µg/g)	$[SO_4^{2-}]$ (µg/g)	Temp. (°C)	E_{CORR} (mV_{SCE})	E_B (mV_{SCE})	E_{RP} (mV_{SCE})	$(E_B - E_{RP})$ (mV)
6	85	20	30	–245	–	–	–
6	**8500**	**20**	**30**	**–221**	**864**	**839**	**25**
1000	85	20	30	–231	–62	–62	0
1000	**8500**	**20**	**30**	**–210**	**855**	**367**	**488**
6	85	1000	30	–143	82	109	–27
6	**8500**	**1000**	**30**	**–212**	**329**	**73**	**256**
1000	85	1000	30	–245	–36	–36	0
1000	**8500**	**1000**	**30**	**–201**	**312**	**72**	**240**
6	**85**	**20**	**95**	**–288**	**325**	**421**	**–96**
6	8500	20	95	–231	630	630	0
1000	85	20	95	–345	–64	–64	0
1000	8500	20	95	–406	591	591	0
6	85	1000	95	–355	102	–50	152
6	8500	1000	95	–284	617	617	0
1000	85	1000	95	–348	–47	24	–71
1000	8500	1000	95	–404	633	633	0

the absence of these factors, pits on copper tend to die (or re-passivate). Factors that lead to pit death include: (a) blockage of the cathode surface by the precipitation of $CaCO_3$ or other non-conducting corrosion products, (b) the opening of the occluded cell by fracture of the cap of corrosion products, allowing mixing of the pit and bulk solutions, and (c) coalescence of adjacent pits. Each of these factors results in an increase in the anodic:cathodic surface area ratio. There is evidence for a maximum diameter of isolated pits on copper of 0.1–0.5 mm. Above this diameter, pits will tend to coalesce and the surface become roughened as opposed to pitted.

3.2 Stress corrosion cracking

3.2.1 Initiation

Stress corrosion cracking (SCC) is the result of the conjoint action of a tensile stress on a susceptible material in an aggressive environment. Therefore, it is useful to consider aspects of both the initiation and propagation of SCC in terms of material, mechanical, and environmental factors.

Relatively little information is available regarding the effects of material properties of pure copper on the initiation of SCC /King et al, 2001/. Of those studies that have been performed, the only ones relevant to the initiation of SCC as a result of surface discontinuities or changes in material properties due to welding involve the effect of grain size. Cracks inevitably initiate intergranularly at grain boundaries, even in environments in which crack growth is transgranular. Thus, larger grained material, as might result from grain growth during welding, exhibits a lower density of initiated cracks /Pugh et al, 1969; Yu et al, 1987/.

Surface discontinuities could promote SCC initiation through their effect as stress intensifiers. Discontinuities exhibiting sharp crack-like features, such as that shown in Figure 2-2f, affect the stress intensity factor (K_I) at the crack tip. For blunt discontinuities or pits, such as those shown in Figure 2-2c and e, the appropriate measure is the stress concentration factor /Pilkey, 1997/. The effect of crack-like and blunt discontinuities can then be determined by comparison with threshold stress intensity factors or threshold stresses for crack initiation.

Various authors have tried to determine the threshold stress intensity factor for SCC (K_{ISCC}) in OF-Cu /King et al, 2001/. Figure 3-11 shows data from /Pettersson and Oskarsson, 2000/ for OF-Cu in sodium nitrite solution that suggests a K_{ISCC} value of ~ 30 MPa·$m^{1/2}$. In order to observe any crack growth, these authors found it necessary to introduce cold work to strengthen the material, the opposite of the material softening likely to result from the final closure weld. For annealed OF-Cu, /King et al, 1999/ suggested a threshold stress intensity factor of ~ 22 MPa·$m^{1/2}$. However, reviewing the data from these studies and that of /Hietanen et al, 1996/, /Rosborg and Werme, 2001/ noted that the variability in reported K_{ISCC} values (from 16 to 30 MPa·$m^{1/2}$) makes it difficult to define a single value for life prediction purposes.

There are a number of measurements of the threshold stress for the initiation (and growth) of SCC cracks reported in the literature /King et al, 2001/. /Saario et al, 1999/ reported a threshold stress of 120 MPa for copper in sodium nitrite solution. /Sato and Nagata, 1978/ found that the threshold stress in ammonia environments was a function of the phosphorus content of the material. Below a P content of ~ 80 ppm, the threshold stress was > 200 MPa, but diminished considerably for P contents of between 80 and 250 ppm to a value of ~ 40 MPa. The P content of the OF-Cu to be used to fabricate canisters is likely to be of the order of ~ 50 ppm /Werme, 1998/, so that the threshold stress for SCC for a canister will be ≥ 120 MPa.

Another impact of the applied stress is the accompanying strain. As noted by /Parkins, 1985/, the strain that results from the applied stress is likely to be equally or more important for crack initiation and growth than the stress itself. Strain, especially local plastic deformation, is responsible for the rupture of protective oxide films at grain boundaries or at the crack tip.

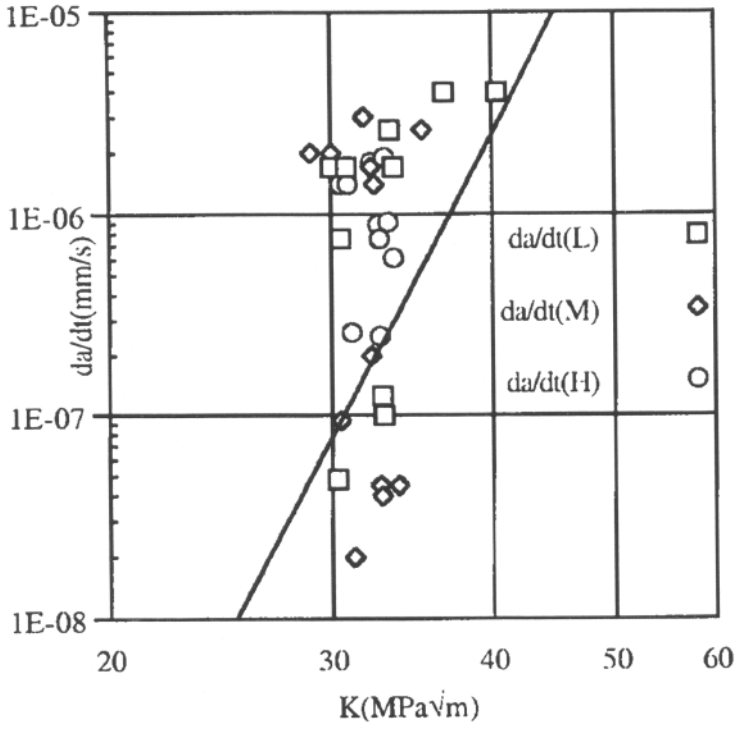

Figure 3-11. *Effect of stress intensity factor on the crack growth rate for OF-Cu in sodium nitrite solution /Pettersson and Oskarsson, 2000/.*

/Sieradzki and Kim, 1992/ observed a dynamic interaction between the strain rate and the rate of dissolution of Cu in ammonia solutions. These authors were able to initiate transgranular SCC of copper in ammonia solutions via a film-induced cleavage mechanism for certain combinations of the rate of dissolution and the strain rate. Under these conditions, a micro-pitted surface layer was produced, the fracture of which was able to sustain crack propagation into the underlying ductile base material. However, the scale of the porosity and the properties of this surface film are crucial in determining whether SCC will occur /Sieradzki and Newman, 1985/, and the macro-porosity resulting from welding discontinuities would not support crack initiation via this mechanism.

Environmental factors are clearly important in the initiation (and growth) of cracks, since SCC has only been observed on OF-Cu in the presence of certain specific species and over well-defined ranges of electrochemical potential /King et al, 2001/. These environments (nitrite, ammonia, and acetate) exhibit the required combination of film-formation and dissolution necessary for crack initiation. Perhaps the most important property of the environment with respect to crack initiation, is the formation of a protective film. Cracking is only observed in these solutions at combinations of potential and pH at which a Cu_2O (or $Cu_2O/Cu(OH)_2$) film is stable /Benjamin et al, 1988; Cassagne et al, 1990; Suzuki and Hisamatsu, 1981/.

In addition to considering the separate effects of material, mechanical, and environmental factors, it is worth considering the effects of pits, which have a special relationship to the initiation of SCC. Much of the evidence linking pitting to crack initiation comes from studies on materials other than copper alloys, in particular the numerous studies of the SCC of C-steels. However, the possibility that a similar link may also exist for OF-Cu is illustrated by the data in Figure 3-12. This figure shows a comparison of the pitting (or breakdown) potential E_B measured in acetate solution in the absence of Cl^- ions /Laz et al, 1992/ and "threshold" potentials for SCC measured on smooth tensile samples using slow strain rate testing in acetate and nitrite solution. (These "threshold" potentials are simply potentials below which SCC was not observed on laboratory timescales, and may or may not represent a true mechanistic threshold for SCC). Slow strain rate testing on smooth samples involves both the initiation and propagation of cracks, although opinions differ of the relative importance of each process in the overall test. There appears to be a close correlation between E_B and E_{SCC}, although whether this is because cracks are initiated from pits or whether both processes involve the breakdown of a $Cu_2O/Cu(OH)_2$ surface film is uncertain.

Two distinct mechanisms have been proposed to explain the role of pits in crack initiation /Parkins, 1985/. Pits, along with other notch-like features, act as stress raisers /Pilkey, 1997/ and may concentrate the applied stress so that it exceeds a critical threshold stress for crack initiation. Strong evidence linking the stress intensification by pits to the initiation of SCC on C-steel has been presented by /Christman, 1990/, amongst others. A second, less obvious, effect of pits is to alter the composition of the environment and the potential of the surface in localised occluded regions. /Parkins, 1985/ has suggested that this latter effect is more important than the stress intensification effect under some circumstances. As discussed in Section 3.1.2, however, there may be an upper limit to the dimension at which a pit can still affect the local environment.

In summary, like pit initiation, the initiation of SCC cracks occurs at a microscopic level, generally at grain boundaries or other sub-grain size features, such as slip steps. The presence of a surface film (most likely possessing a duplex $Cu_2O/Cu(OH)_2$ structure) appears an important pre-requisite for cracking.

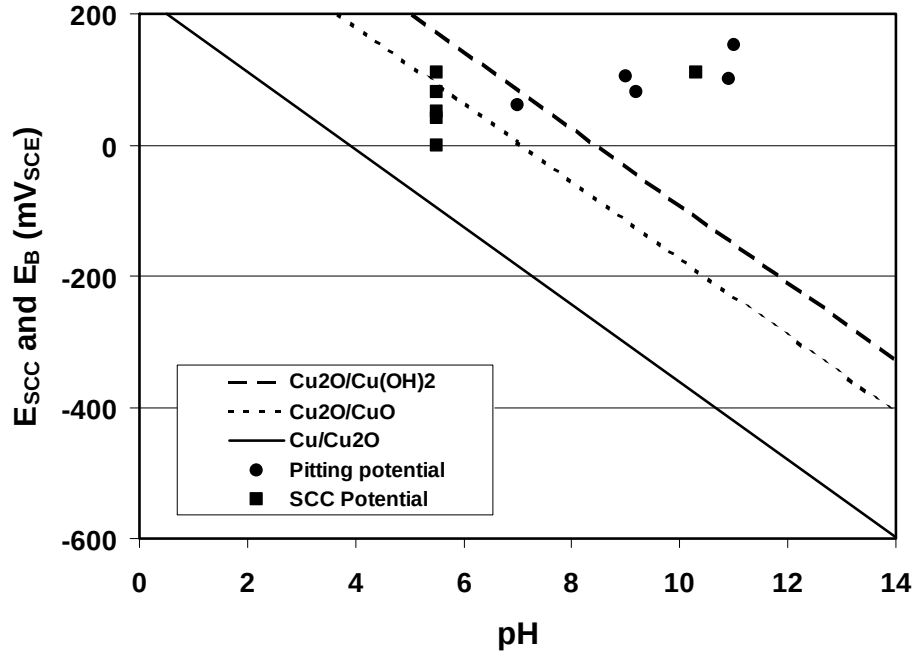

(a) Pitting and cracking potentials in acetate solutions.

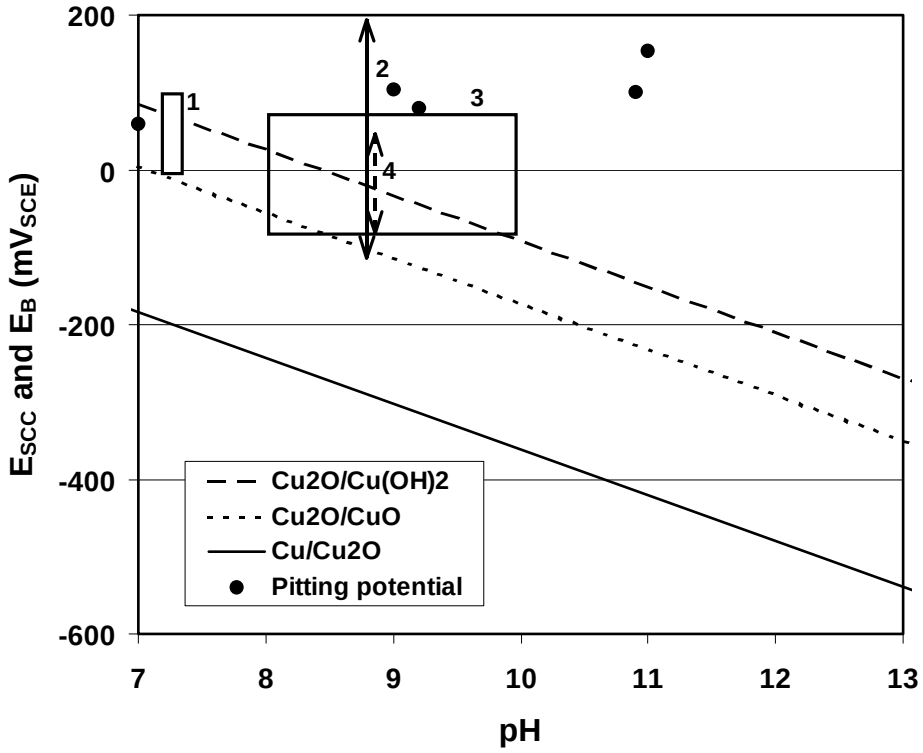

(b) Pitting potentials in acetate and cracking potentials in nitrite solutions. E_{SCC} determined by 1: /Uchida et al, 1991/, 2: /Yu and Parkins, 1987/, 3: /Benjamin et al, 1988/, 4: /Cassagne et al, 1990/.

Figure 3-12. *Comparison of pitting (breakdown) potentials measured in acetate solutions and potentials for SCC on smooth tensile samples determined in acetate and nitrite solutions.*

3.2.2 Propagation

Many of the same factors that are important for crack initiation are also important for crack propagation. To some extent this conclusion arises from the difficulty of distinguishing crack initiation from crack propagation. Crack growth requires a specific environment acting on a susceptible material under a tensile stress. The various mechanisms used to describe crack propagation on copper have been described in more detail elsewhere /King et al, 2001/. Here, only two aspects of crack growth will be considered; crack chemistry and the effects of strain and strain rate on crack growth.

For many SCC systems, a significant difference in chemistry develops between the environment inside the crack and that in the bulk. Differences in chemistry can arise from the acidification of the crack solution by the hydrolysis of dissolved metal ions, in much the same way that acidic pit and crevice chemistries develop in localised corrosion. Potential gradients along the crack can result in significant differences in potential between the crack tip and the crack mouth. Both hydrolysis and the potential gradient will cause an increase in the concentrations of anions (most likely chloride or sulphate) inside the crack. These differences might be enhanced, or sustained, by pre-existing surface discontinuities.

Of the various mechanisms proposed for crack growth of OF-Cu, the most generally accepted (the film rupture/anodic dissolution and tarnish-rupture mechanisms) involve preferential dissolution at the crack tip /King et al, 2001/. To sustain growth, the crack chemistry must support not only dissolution at the crack tip but also passivation of the crack walls, so that the crack remains sharp and does not become blunted. For such mechanisms, however, there is little driving force for the development of potential and concentration gradients along the crack. As stated above, the crack walls must be passive to avoid blunting, so the current flowing along the crack is necessarily small. Thus, the transport of anions into the crack by electro-migration is also minimal. Copper will dissolve as cuprous species, which do not hydrolyse strongly, especially in the presence of chloride ions. Therefore, local acidification will also be minimised. The crack environment, therefore, will be similar to the bulk environment, so that even if surface discontinuities were to exacerbate any differences in the conditions inside the crack, these differences are likely to be small for OF-Cu.

A second effect that surface discontinuities might have on the propagation of cracks in OF-Cu is the enhancement of stress at the crack tip. For dissolution-based mechanisms involving rupture of a surface film, however, the resultant strain is more important than the stress itself. For crack propagation, it is generally found that the rate of change of strain is the more-important parameter /Parkins 1985, 1988/, since crack advance is a balance between the rate of dissolution and the rate of rupture of the film. Strain may result from creep of the material. Although creep could rupture protective films resulting in crack growth (or initiation), it could also blunt cracks by relieving the stress at the crack tip. Stress relief through creep is more likely at higher temperatures. There is evidence from the work of /Pettersson and Oskarsson, 2000/ that crack-tip creep slows crack growth since, under constant load conditions, the crack growth rate decreased with time. Creep exhaustion is commonly postulated as the cause of crack dormancy in C-steels /Parkins, 2000/. Thus, enhancement of the crack-tip strain or strain rate by surface discontinuities may lead to crack dormancy because of the stress relief promoted by creep.

3.3 The effect of surface finish

Although not directly related to the effect of surface discontinuities on localised corrosion and SCC, the effect of the surface finish on these processes is also of interest. The current specification for the surface finish on canisters is DIN ISO 1302 N9, which corresponds to a surface texture of 6.3 µm (the mean distance between the median surface height and the various peaks and troughs).

/Raicheva, 1984/ studied the effect of surface preparation on the electrochemical behaviour of pure copper in acidic O_2-containing KCl solution. Surfaces were prepared by either sequential mechanical polishing to final grit sizes varying from 42 µm to 210 µm or by chemical or electrochemical polishing techniques. The only effect of the mechanical polishing (which, of those studied, most-closely corresponds to the type of surface preparation for the canister) was on the effective surface area for the anodic and cathodic reactions. By correcting for the differences in surface area for the different grit sizes, /Raicheva, 1984/ was able to show that other effects, such as the local surface plastic deformation introduced by polishing, had no effect on the rate of hydrogen evolution in acidified 1 $mol \cdot dm^{-3}$ KCl solution. Although no dissolution data were presented, it was implied that the difference in effective surface area was also the only effect of polishing on the anodic kinetics.

This latter point is important, since it allows the effect of surface finish on the corrosion potential E_{CORR} to be predicted. If the effective surface areas for the anodic and cathodic reactions are equally affected by mechanical polishing, then E_{CORR} will not be a function of the surface roughness. This is important, since it means that local galvanic cells will not be established on different parts of the surface that exhibit different degrees of surface roughness. Therefore, the surface finish will not affect the probability of the initiation of localised corrosion or SCC.

4 Discussion of the effects of discontinuities on the corrosion behaviour of copper canisters

4.1 General considerations

4.1.1 Discontinuities of relevance to corrosion behaviour of canister

Not all discontinuities will be important for the corrosion behaviour of the canister. Those discontinuities located deep within the canister shell will not impact corrosion processes at any stage during the canister service life. Of most importance are surface-breaking defects. Because of the limited amount of oxidant in the repository, sub-surface discontinuities will be less important. Based on a maximum wall penetration by general and localised corrosion of 2 mm /King et al, 2001/, it can be assumed that sub-surface defects located deeper than 2 mm from the canister surface will never be exposed to the repository environment and will, therefore, not influence the corrosion behaviour of the canister.

4.1.2 Importance of microscopic and macroscopic surface features

It is apparent from the discussion above that the initiation of localised corrosion and stress corrosion cracking occurs on a much smaller physical scale than that represented by weld discontinuities. Pit initiation is a microscopic process, occurring due to the localised breakdown of a protective surface film at grain boundaries (Figures 3-3, 3-4, and 3-5). Similarly, the initiation of SCC invariably occurs at grain boundaries, even in environments that support transgranular crack growth /Pugh et al, 1969; Yu et al, 1987/. Weld discontinuities of the kind illustrated in Figure 2-2, on the other hand, represent a macroscopic scale of defect. Therefore, from the viewpoint of the initiation of localised corrosion and SCC by the breakdown of a protective surface film, the presence of such discontinuities should have no detrimental effect whatsoever.

4.1.3 Effect of evolving redox conditions within the repository

The environmental conditions within the repository will evolve over time from initially warm and oxidising to ultimately cool and anoxic /King et al, 2001/. Both localised corrosion and SCC are generally associated with oxidising environments. It is reasonable to assume, therefore, that any impact of discontinuities on the corrosion behaviour of the canister will only be felt during this initial oxidising period.

The importance of the evolution of the repository environment can be illustrated by considering the processes determining the propagation (and death) of pits. The requirements for pit growth include:

1. Permanent separation of anodic and cathodic sites.
2. Anodic current density in the occluded region must be greater than that on the exposed surface.

Under oxidising conditions, these two criteria are generally met through the creation of an occluded region capped by a layer of precipitated corrosion products (see, for example, Figures 3-3 to 3-6). Pit growth will continue as long as the flux of O_2 to the external surface

is maintained (provided the pit does not grow too wide that the cap of precipitated corrosion products cannot be sustained in which case the pit will die, Figure 3-5 f).

Under anoxic conditions, however, it will be difficult to sustain the anodic reaction in the occluded region. In the presence of sulphide (HS^-) the anodic reaction is /King et al, 2001/

$$2Cu + HS^- \rightarrow Cu_2S + H^+ + 2e^- \quad (4\text{-}1)$$

There is evidence that the rate of the anodic reaction is limited by the rate of supply of HS^- to the copper surface /King et al, 2001/; (D W Shoesmith, private communication 2003). It is physically impossible to sustain a localised process in an occluded region if the anodic reaction is mass-transport controlled by the supply of a reactant from the bulk environment. Under these circumstances, the rate of supply of HS^- to the pit would be significantly smaller than to the exposed surface, so that the second criterion for pit growth listed above cannot be maintained.

Therefore, the effects of localised corrosion, and any impact that pre-existing discontinuities may have, is an issue only during the initial oxidising phase of the evolution of the repository environment.

4.2 Localised corrosion

4.2.1 Initiation and propagation

As noted above, pit initiation results from the breakdown of a protective surface film at grain boundaries. The breakdown process can be determined electrochemically through the measurement of the breakdown or pitting potential E_B. In naturally corroding systems, the surface will pit if the corrosion potential E_{CORR} becomes more anodic than E_B. There is no evidence that the presence of pre-existing surface discontinuities affects either E_{CORR} or E_B. In general, the types of discontinuity illustrated in Figure 2-2 are too large to influence an event (i.e. pit initiation) that occurs on the microscopic level.

Similarly, an argument can be made that many of these discontinuities are too large to sustain pit growth. Evidence has been presented in Section 3.1.2 that individual pits exhibit a maximum diameter of 0.1–0.5 mm, and that above this size the individual pits coalesce. Pit coalescence leads to the death of a propagating pit because of the associated increase in the anodic:cathodic surface area ratio (Figure 3-5g). In the repository, this effect will be compounded by the decrease in O_2 flux to the canister surface as the repository environment evolves over time.

Thus, the types of discontinuity shown in Figure 2-2 are too physically too large to cause pit initiation or sustained growth.

4.2.2 Growth of hemispherical discontinuities

Despite the conclusion above that surface discontinuities are too large to lead to sustained pit growth, it is illustrative to consider the maximum possible pit diameter on a canister if sustained growth were possible. Consider a hemispherical surface-breaking discontinuity of initial radius r_1 (Figure 4-1). Let us assume that as the discontinuity grows the hemispherical shape is maintained. Dissolution is supported by the cathodic reduction of O_2 on the external surface surrounding the “pit.” The width of the circular annulus on which the cathodic reaction occurs is r_2, and is determined by the extent to which the anodic and

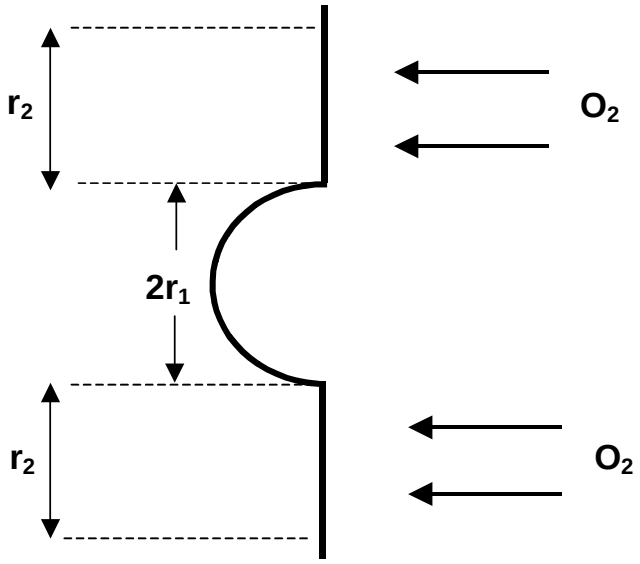

Figure 4-1. *Illustration of an idealised hemispherical surface-breaking discontinuity.*

cathodic reactions can galvanically couple on the surface of a canister embedded in compacted bentonite.

The flux of O_2 to the canister wall is time dependent. The predicted time dependence of the O_2 flux and of the cumulative amount of diffused O_2 (Q_{O2}) is shown in Figure 4-2. These predictions are based on the assumption that the O_2 reduction reaction is transport limited and that all of the O_2 initially in the borehole (both dissolved O_2 and gaseous O_2 in the initially unsaturated pores, initial degree of saturation 60%, porosity 0.41) diffuses through the pore water (assumed diffusion coefficient 1 x 10^{-7} $cm^2 \cdot s^{-1}$). Based on these calculations, ~ 99% of the O_2 is consumed within the first ~ 3000 years, which can be used as a definition of the length of the aerobic phase.

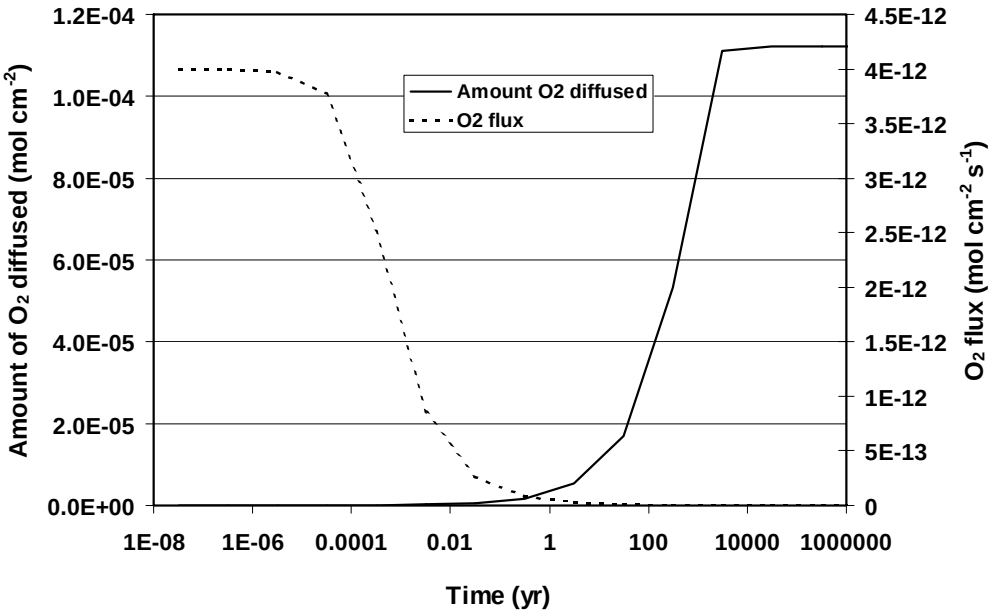

Figure 4-2. *Predicted time dependence of the flux of O_2 to the canister surface and of the time-integrated amount of O_2 that has diffused (see text for details).*

Assuming the pit grows hemispherically from its initial radius r_1, the increase in the pit radius Δr is given by

$$\Delta r = \left(\sqrt[3]{\left(\frac{6A}{\pi\rho} \int Q_{O_2} dr + r_1^3 \right)} \right) - r_1 \qquad (4\text{-}2)$$

where A and ρ are the atomic mass and density of copper, $\int Q_{O_2} dr$ is the spatially integrated cumulative flux of O_2 that supports pit growth, and it is assumed that the reduction of 1 mol O_2 supports the dissolution of 4 mol Cu.

Figure 4-3 shows the predicted maximum pit depth (equal to $\Delta r + r_1$) as a function of the initial radius of the discontinuity. Predictions are shown for various galvanic coupling distances for the cathodic reduction of O_2, ranging from 1 cm to 30 cm. The coupling distance is unknown, but a distance of the order of 10 cm is likely an upper bound in compacted bentonite because of the electrical resistivity of this material. For this coupling distance, discontinuities with an initial radius of 0.1 mm and 1.0 mm grow to a final size of ~ 7.8 mm. A larger 20 mm diameter (10 mm radius) discontinuity grows to ~ 11.4 mm

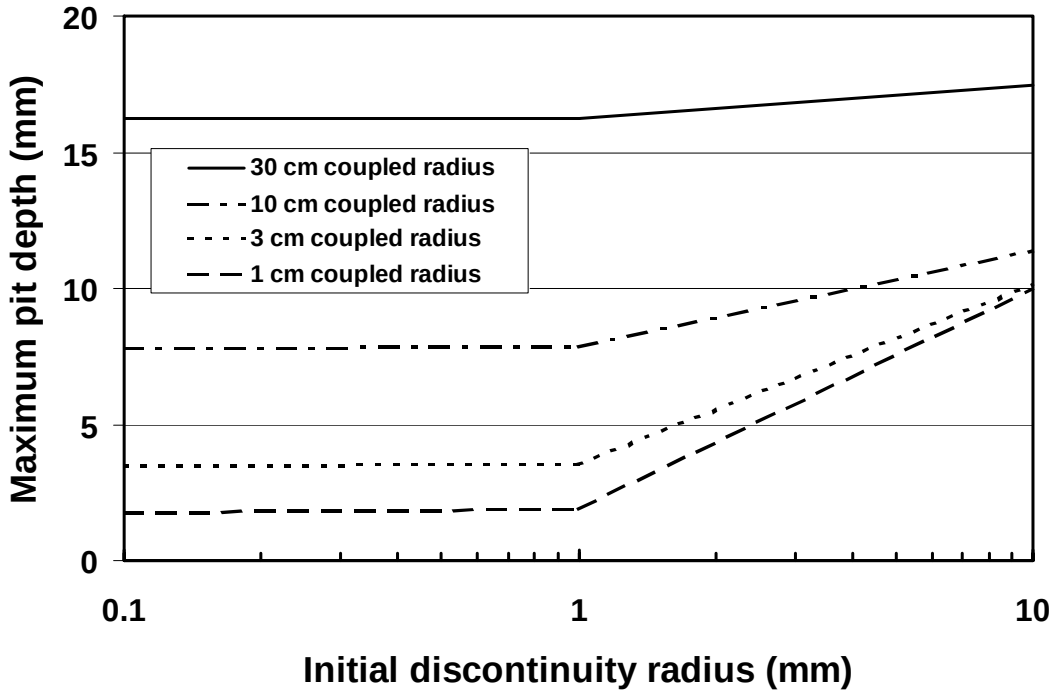

Figure 4-3. *Predicted maximum pit depth (radius) as a function of the initial discontinuity radius for various assumed galvanic coupling distances.*

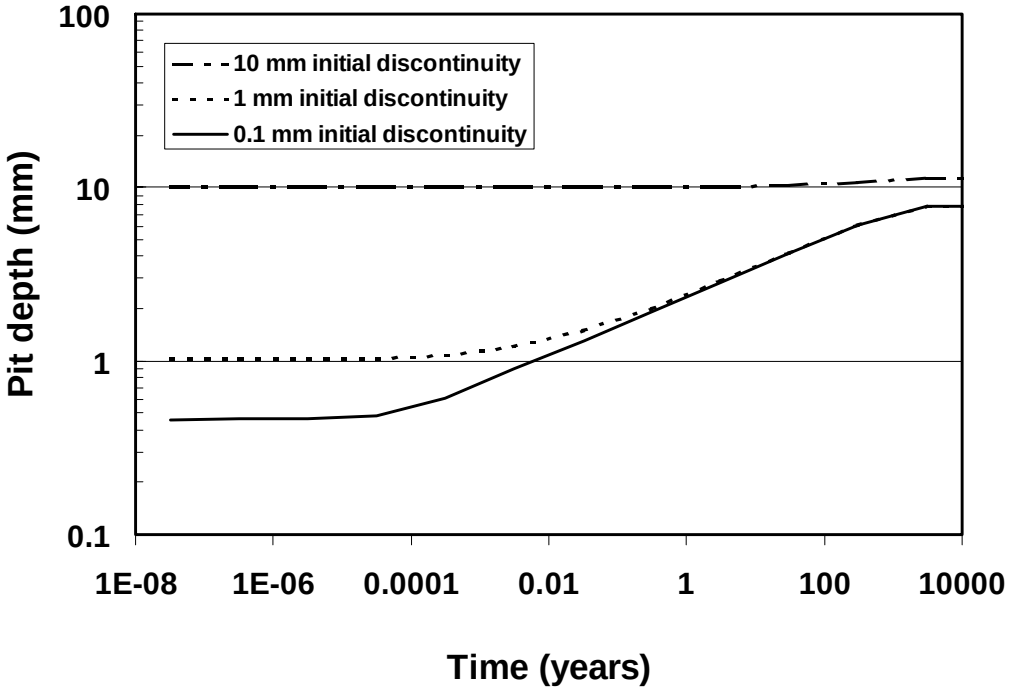

Figure 4-4. *Predicted time dependence of the pit depth (radius) for various initial discontinuity radii for an assumed galvanic coupling distance of 10 cm.*

radius after all the O_2 is consumed. These calculations are highly conservative, since it is assumed that all the O_2 supports pit growth and that none is consumed by the oxidation of pyrite or other oxidisable impurities, by microbial activity, or in the support of general corrosion. Nevertheless, even given such conservative assumptions, the growth of the discontinuity will not lead to canister failure.

Figure 4-4 shows the predicted time dependence of the pit depth (radius) for various initial discontinuity sizes and for an assumed galvanic coupling distance of 10 cm. Pit growth ceases once all of the O_2 is consumed, marking the end of the aerobic phase in the evolution of repository conditions.

As noted above, however, these propagating pits would most likely coalesce and die once they reach a certain size. From the evidence presented above, individual pits coalesce or stop growing once they reach 0.1–0.5 mm in diameter, either as a result of pit opening (Figure 3-5f or pit coalescence (Figure 3-5g), the net result in both cases being an increase in the anodic:cathodic surface area ratio.

4.3 Stress corrosion cracking

4.3.1 Loads experienced by canister

/Lindgren et al, 1999/ have considered the time dependence of the stress and strain of the canister shell as a consequence of external loading and creep processes. The predicted axial and hoop stresses can be used to predict the stress concentration and stress intensification produced by blunt and crack-like discontinuities, respectively. (Although /Lindgren et al, 1999/ also predicted the radial stress, this orientation is of no interest when considering the growth of cracks through the wall of the canister).

For the reference canister design (Figure 1-1) subjected to a bentonite swelling pressure of 15 MPa, the maximum hoop and axial stress near the weld location in the canister shell is in the range 20-40 MPa. Although initially the stresses are generally tensile in the region of the weld, creep tends to induce compressive stresses below the surface. Thus after 10,000 years, both the axial and hoop stresses are compressive at a distance of ~ 20 mm below the surface of the canister shell.

For the current purposes, a maximum tensile stress of 40 MPa is assumed.

4.3.2 Stress concentration by blunt discontinuities

Blunt, surface-breaking defects will concentrate the applied stress which may, if the environment is suitable, lead to the initiation of SCC. /Christman, 1990/ used the following expression to estimate the stress concentration factor (SCF) at the base of surface pits

$$SCF = \left[3\left(\frac{D}{2r} \right)^{1/2} - 1 \right] + \frac{4}{2 + (D/2r)^{1/2}} \qquad (4\text{-}3)$$

where D is the pit depth and r is the pit (root) radius.

Figure 4-5 shows the variation in SCF with discontinuity depth for various discontinuity radii. As would be expected, the stress concentration increases with increasing depth and decreases with increasing bluntness (increasing radius) of the base of the discontinuity.

Other estimates for the SCF for various geometries are given by /Pilkey, 1997/. For a hemispherical pit under biaxial stress, /Pilkey, 1997/ reports a value of 2.23 for the SCF, somewhat smaller than the value of 3.33 predicted from Equation (4-3). For elliptically shaped surface-breaking discontinuities, /Pilkey, 1997/ reports a value of 3.4–3.8.

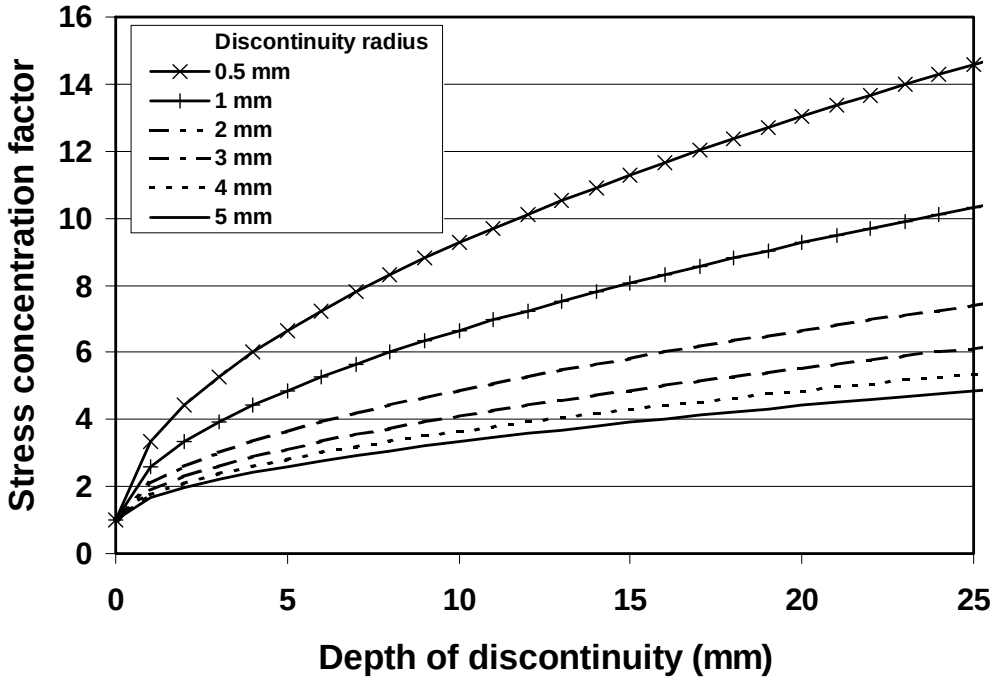

Figure 4-5. *Variation in stress concentration factor with depth for various size discontinuities, after /Christman, 1990/.*

The SCF for the discontinuities shown in Figure 2-2 can be estimated based on Equation (4-3). The lowest SCF are found for the "rounder" discontinuities, such as those in Figures 2-2c and 2-2e (SCF = 4.1). The more elongated discontinuities in Figures 2-2a and 2-2f produce the highest SCF of ~ 5.4.

The maximum stress can be calculated based on these SCF values and the canister wall stresses predicted by /Lindgren et al, 1999/. For a tensile stress of 40 MPa, the maximum stress at the base of a discontinuity is likely to be of the order of 160–200 MPa. These values are halved for surface stresses of 20 MPa, as are likely after the canister shell has undergone creep. Nevertheless, for some period of time, the maximum stress could exceed the threshold stress for SCC of ~ 120 MPa (see Section 3.2.1). Crack initiation, however, also requires the presence of the correct environment and electrochemical potential. After stress relaxation following creep of the canister shell, crack initiation at the base of discontinuities seems unlikely even in the presence of an appropriate environment.

4.3.3 Stress intensification by crack-like discontinuities

For crack-like defects, the appropriate measure of the effect of the discontinuity is the crack-tip stress intensity factor K_I. Fracture mechanics solutions to many crack geometries are now available /Murakami, 1987/. By way of example, consider a single edge crack in a semi-infinite plate subject to a uniaxial tensile stress σ (Figure 4-6). The stress intensity factor is given by /Murakami, 1987/

$$K_I = 1.1215\sigma(\pi a)^{1/2} \qquad (4\text{-}4)$$

where a is the crack depth.

When combined with the stress values predicted by /Lindgren et al, 1999/, Equation (4-4) can be used to predict the crack-tip stress intensity factor for crack-like discontinuities in the canister shell. Figure 4-7 shows the predicted K_I as a function of crack depth for various stresses. For the maximum axial or hoop stress of 40 MPa, the discontinuity would have to be nearly through-wall for the stress intensity factor to exceed the lowest reported K_{ISCC} value. For the lower stress level following creep of the canister shell (20 MPa), even a through-wall crack-like discontinuity would not exceed K_{ISCC}. Furthermore, this analysis does not take into account the generation of sub-surface compressive stresses following creep deformation.

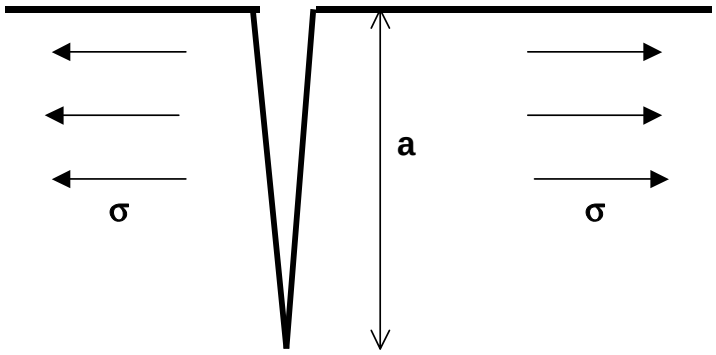

Figure 4-6. *Schematic illustration of an edge crack in a semi-infinite plate subject to uniaxial tensile loading.*

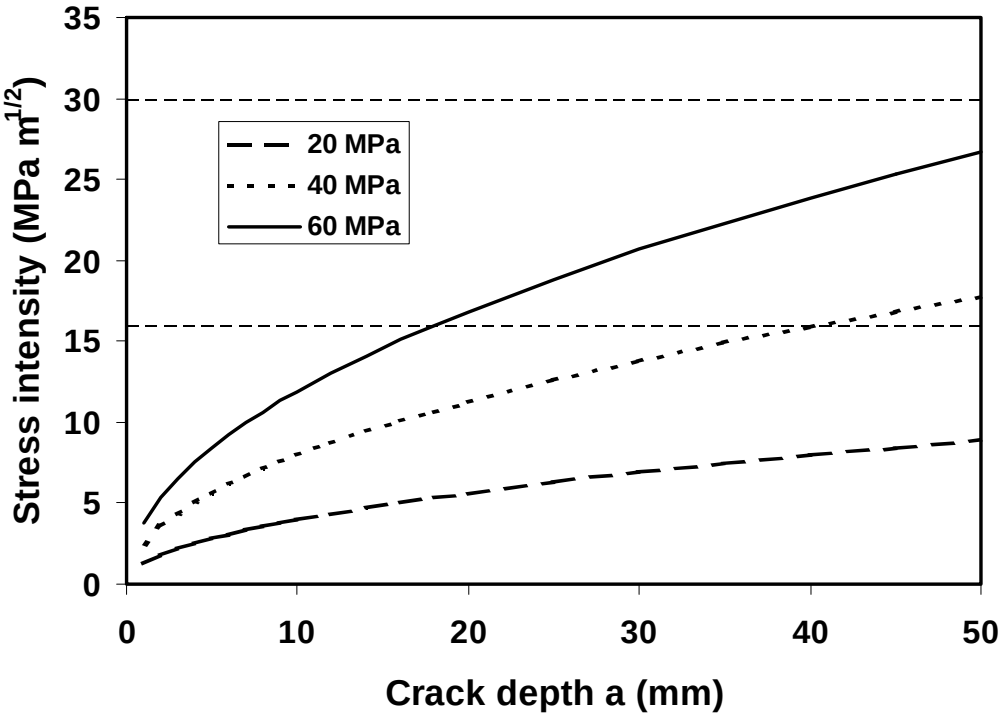

Figure 4-7. *Variation in stress intensity factor for a single edge crack in a semi-infinite plate as a function of crack depth for various uniaxial stresses. Also shown on the figure is the range of threshold stress intensity factors for SCC (K_{ISCC}) of OF-Cu in nitrite solution.*

Multiple edge cracks shield each other from the applied stress, resulting in lower K_I values than for a single crack /Murakami, 1987/.

Based on the evidence from Figure 2-2, crack-like discontinuities are uncommon. Figure 2-2f, however, appears to show a crack-like feature at the base of a lens-shaped discontinuity. /Murakami, 1987/ presents a solution for a crack at the base of a triangular notch subject to uniaxial tensile loading (Figure 4-8). The crack tip stress intensity factor is a function of the combined depths of the notch and crack (a + b), of the ratio of the crack:notch depths (b/a), and of the angle at the base of the notch (β) /Murakami, 1987/.

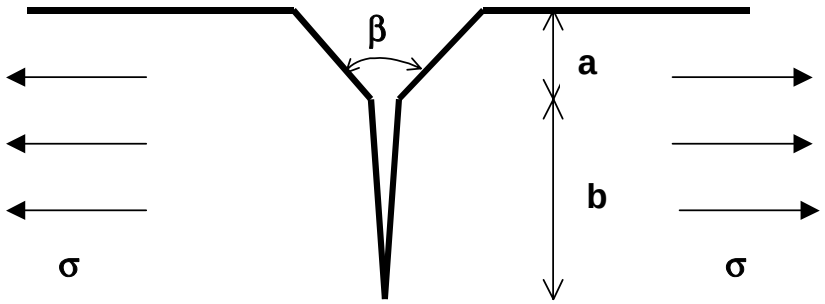

Figure 4-8. *Schematic of a crack (depth b) emanating from the base of a triangular notch (depth a, notch angle β) and subject to uniaxial tensile stress σ.*

Figure 4-9 shows the variation of K_I as a function of the combined depth of the notch and crack for various tensile stresses. These data were calculated for the worst case of a high crack:notch depth ratio (b/a) and for acute notch angles (< 90°). Nevertheless, the predicted K_I does not exceed the minimum observed K_{ISCC}, except for extreme applied stresses or for very long discontinuities. As for the single edge crack, therefore, crack growth from a crack-like discontinuity at the base of a notch on the canister surface seems unlikely.

The effect of the crack:notch depth ratio on K_I is shown in Figure 4-10. The stress intensity is smaller for short cracks. For crack lengths that do not exceed 50 of the notch depth, the stress intensity factor is lower than the smallest reported value of K_{ISCC} for all sizes of discontinuity. Thus, for the crack-like feature at the base of the discontinuity in Figure 2-2f (b/a = 0.125), the crack-tip stress intensity factor would be < 12 MPa·m$^{1/2}$ regardless of the depth of the discontinuity.

Finally, Figure 4-11 shows the effect of notch angle on the crack-tip stress intensity factor. More acute notches lead to higher K_I, whereas discontinuities with rounder bases exhibit lower K_I values.

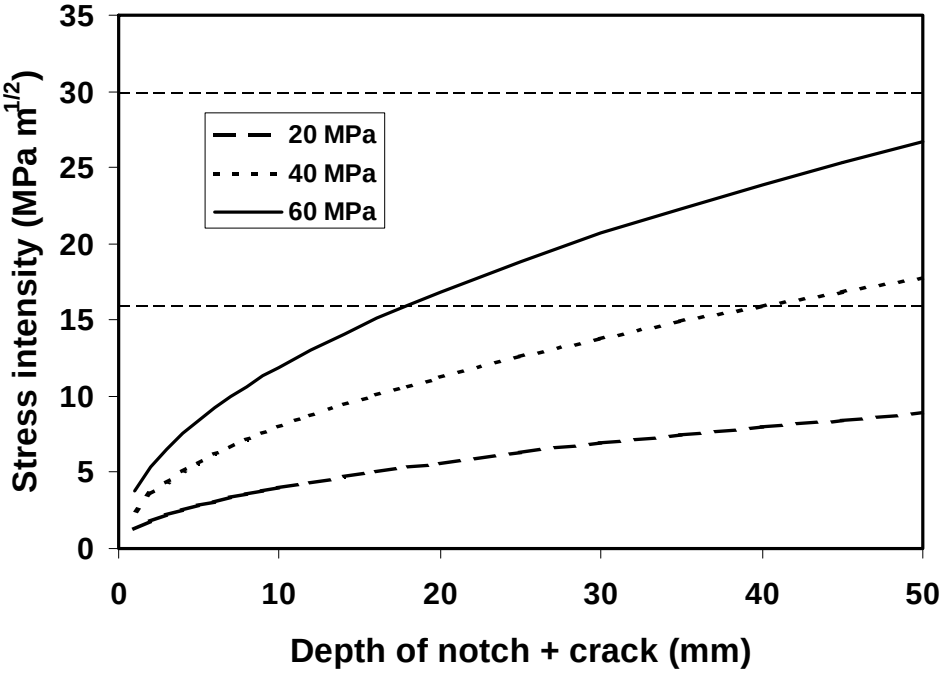

Figure 4-9. *Predicted crack-tip stress intensity factor for a crack at the base of a triangular notch for various applied stress levels. Values shown for a high crack:notch depth ratio and an acute notch angle. Also shown on the figure is the range of threshold stress intensity factors for SCC (K_{ISCC}) of OF-Cu in nitrite solution.*

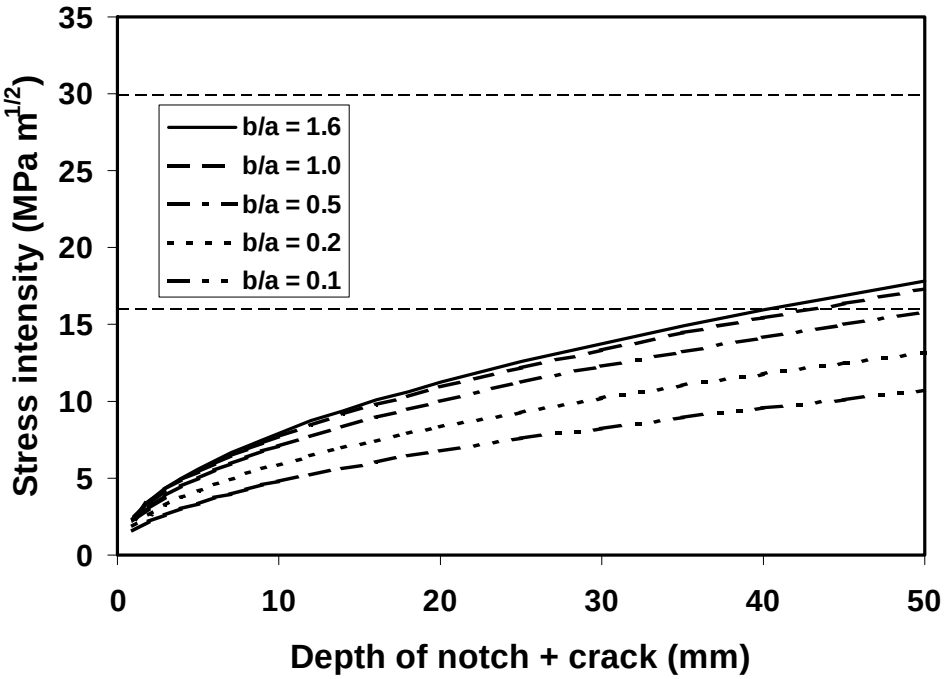

Figure 4-10. *Predicted crack-tip stress intensity factor for a crack at the base of a triangular notch for various crack:notch depth ratios (b/a). Values shown for an applied stress of 40 MPa and a notch angle of 160°. Also shown on the figure is the range of threshold stress intensity factors for SCC (K_{ISCC}) of OF-Cu in nitrite solution.*

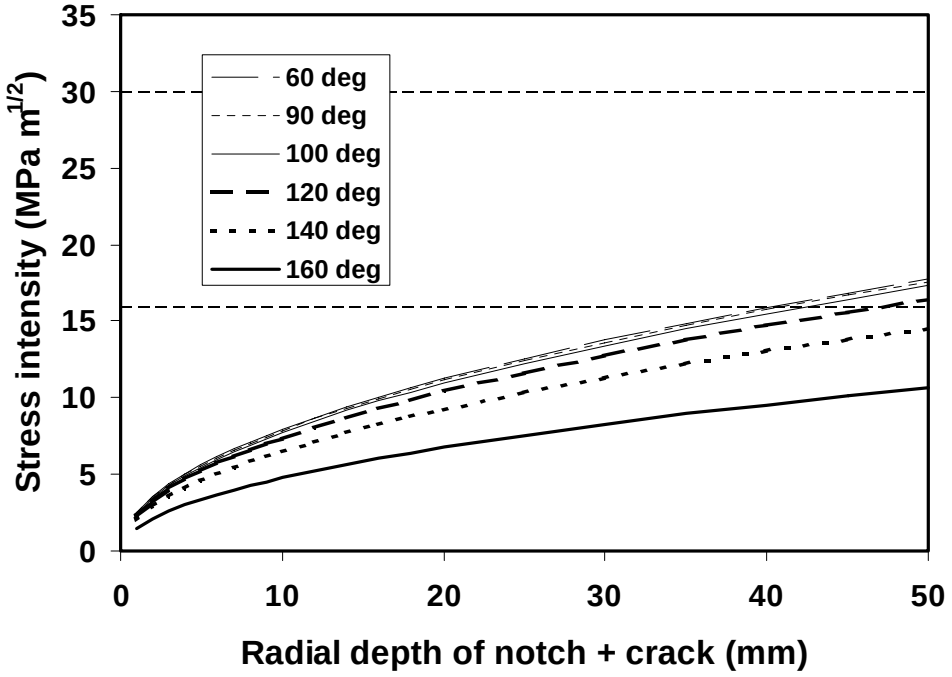

Figure 4-11. *Predicted crack-tip stress intensity factor for a crack at the base of a triangular notch for various notch angles. Values shown for an applied stress of 40 MPa and a crack:notch depth ratio of > 1.6. Also shown on the figure is the range of threshold stress intensity factors for SCC (K_{ISCC}) of OF-Cu in nitrite solution.*

4.4 Impact of discontinuities on the service life of copper canisters

4.4.1 Localised corrosion

It is unlikely that the presence of pre-existing surface-breaking discontinuities will impact the service life of the canister as a result of localised corrosion. As stated above, discontinuities will not act as preferential sites for pit initiation, which instead occurs at grain boundaries due to the localised breakdown of protective surface films. Environmental factors and the presence of a defected film are more important for pit initiation than the presence of a pit-shaped discontinuity.

Similarly, the presence of pre-existing pit-shaped discontinuities is not likely to lead to the growth of deep pits. Acute pits (i.e. those with small width:depth ratios) are not observed on copper, which instead tends to exhibit hemispherical or shallower pits. There is evidence that the pit shape is influenced by the ability to maintain an occluded cell under a cap of precipitated corrosion products. For copper, the maximum diameter of isolated pits is of the order of 0.1–0.5 mm. Above this size, pits tend to coalesce, which inevitably results in more general corrosion of the surface. Combined with the tendency for pits to die as the supply of oxidant diminishes (as will happen in the repository), these observations support the contention that discontinuities with an initial diameter of > 0.5 mm will not grow deeper by localised corrosion.

4.4.2 Stress corrosion cracking

Surface discontinuities can influence the corrosion behaviour through concentration or intensification of applied stresses or through effects on the local environment. A quantitative assessment of the latter effect lies outside the scope of this study. However, the predicted E_{CORR} of a canister (maximum –250 mV_{SCE}, /King et al, 2001/) lies several hundred mV below the threshold potentials for SCC in Figure 3-12. Since there is no apparent mechanism for the ennoblement of E_{CORR} due to surface discontinuities, it appears than SCC of copper canisters can be ruled out on environmental grounds alone.

Quite apart from any environmental consideration, it would also appear that SCC is unlikely due to stress concentration or intensification by surface-breaking discontinuities. For blunt or round-bottomed discontinuities, stress concentration effects may lead to stresses that exceed the apparent threshold stress for SCC. However, if a crack does initiate at the base of a notch then the predicted stress intensity factor is too low to support crack growth, especially for short, newly initiated, cracks. Therefore, cracks will go dormant, an effect that will be compounded by creep at the crack tip (which will tend to reduce crack-tip stresses) and the presence of local compressive stresses beneath the canister wall. A similar situation applies to pre-existing crack-like discontinuities. All the evidence presented here suggests that the crack-tip stress intensity factor will be below the minimum K_{ISCC} value reported in the literature.

5 Summary and conclusions

The relevant literature on the initiation and propagation of localised corrosion and SCC has been reviewed. Initiation of localised corrosion occurs at the microscopic scale at grain boundaries, and will not be affected by the presence of macroscopic discontinuities. The localised breakdown of a passive $Cu_2O/Cu(OH)_2$ film at a critical electrochemical potential determines where and when pits initiate, not the presence of pit-shaped surface discontinuities.

The factors controlling pit growth and death are well understood. There is evidence for a maximum pit radius for copper in chloride solutions, above which the small anodic: cathodic surface area ratio required for the formation of deep pits cannot be sustained. This maximum pit radius is of the order of 0.1–0.5 mm. Surface discontinuities larger than this size are unlikely to propagate as pits, and pits generated from smaller discontinuities will die once they reach this maximum size. Death of propagating pits will be compounded by the decrease in oxygen flux to the canister as the repository environment becomes anoxic.

Surface discontinuities could impact the SCC behaviour either through their effect on the local environment or via stress concentration or intensification. There is no evidence that surface discontinuities will affect the initiation of SCC by ennoblement of the corrosion potential or the formation of locally aggressive conditions.

Stress concentration at pits could lead to crack initiation under some circumstances, but the stress intensity factor for the resultant cracks, or for pre-existing crack-like discontinuities, will be smaller than the minimum threshold stress intensity factor (K_{ISCC}) for copper reported in the literature. Therefore, any cracks that do initiate will tend to become dormant.

In summary, there is no evidence that weld discontinuities will adversely affect the localised corrosion or SCC behaviour of copper canisters. The predicted service life of the canisters is not affected by the presence of such features.

References

Al-Kharafi F M, Shalaby H M, Gouda V K, 1989. Pitting of copper under laboratory and field conditions. Br. Corros. J. 24, 284–290.

Benjamin L A, Hardie D, Parkins R N, 1988. Stress corrosion resistance of pure coppers in ground waters and sodium nitrite solutions. British Corrosion 23, 89–95.

Cassagne T B, Kruger J, Pugh, E N, 1990. Role of the oxide film in the transgranular stress corrosion cracking of copper. In Environmentally Assisted Cracking: Science and Engineering, ASTM-STP-1049, (W.B. Lisagor, T.W. Crooker and B.N. Leis, Editors), American Society for Testing and Materials, Philadelphia, PA, pp. 59–75.

Campbell H S, 1974. A review: pitting corrosion of copper and its alloys. In Localized Corrosion, (Editors, R.W. Staehle, B.F. Brown, J. Kruger and A. Agrawal), NACE International, Houston, TX, pps. 625–638.

Christman T K, 1990. Relationship between pitting, stress, and stress corrosion cracking of line pipe steels. Corrosion 46, 450–453.

de Chialvo M R G, Salvarezza R C, Vasquez Moll D, Arvia A J, 1985. Kinetics of passivation and pitting corrosion of polycrystalline copper in borate buffer solutions containing sodium chloride. Electrochimica Acta 30, 1501–1511.

Hietanen S, Ehrnstén U, Saario T, 1996. Environmentally assisted cracking behaviour of copper in simulated ground water. Finnish Centre for Radiation and Nuclear Safety Report, STUK-YTO-TR 105.

King F, Litke C D, Ikeda B M, 1999. The effect of oxidant supply and chloride ions on the stress corrosion cracking of copper. Ontario Power Generation, Nuclear Waste Management Division Report 06819-REP-01200-10013-R00.

King F, Kolar M, 2000. The copper container corrosion model used in AECL's second case study. Ontario Power Generation, Nuclear Waste Management Division Report 06819-REP-01200-10041-R00. Toronto, Ontario.

King F, Ahonen L, Taxén C, Vuorinen U, Werme L, 2001. Copper corrosion under expected conditions in a deep geologic repository. SKB TR-01-23. Svensk Kärnbränslehantering AB.

King F, 2002. Corrosion of copper in alkaline chloride environments. SKB TR-02-25. Svensk Kärnbränslehantering AB.

Laz M M, Souto R M, Gonzalez S, Salvarezza R C, Arvia A J, 1992. Pitting corrosion of polycrystalline annealed copper in alkaline sodium perchlorate solutions containing benzotriazole. J. Appl. Electrochem. 22, 1129–1134.

Lindgren L-E, Häggblad H-Å, Josefson L, Karlsson L, 1999. Thermo-mechanical FE-analysis of residual stresses and stress redistribution in butt welding of a copper canister for spent nuclear fuel. Proc. Int. Conf. On Structural Mechanics in Reactor Technology, SmiRT-15, Seoul, Korea, Aug 15–20, 1999.

Lucey V F, 1967. Mechanism of pitting corrosion of copper in supply waters. British Corrosion Journal 2, 175–185.

Mankowski G, Duthil J P, Giusti A, 1997. The pit morphology on copper in chloride- and sulphate-containing solutions. Corrosion Science 39, 27–42.

Murakami Y, 1987. Stress Intensity Factors Handbook. Pergamon Press (Oxford, UK).

Parkins R N, 1985. Significance of pits, crevices, and cracks in environment-sensitive crack growth. Mater. Sci. Tech. 1, 480–486.

Parkins R N, 1988. Localized corrosion and crack initiation. Mater. Sci. Eng. A103, 143–156.

Parkins, R N, 2000. A review of stress corrosion cracking of high pressure gas pipelines. CORROSION/2000, National Association of Corrosion Engineers (Houston, TX), Paper No. 363.

Pettersson K, Oskarsson M, 2000. Stress corrosion crack growth in copper for waste canister applications. In Scientific Basis for Nuclear Waste Management XXIII, (R.W. Smith and D.W. Shoesmith, Editors), Material Research Society Proceedings, Volume 608, Pittsburgh, PA, 95–101.

Pilkey W D, 1997. Peterson's Stress Concentration Factors. Second Edition. John Wiley & Sons (New York, NY).

Pugh E N, Craig J V, Sedriks, A J, 1969. The stress-corrosion cracking of copper, silver and gold alloys. In Fundamental Aspects of Stress Corrosion Cracking (R.W. Staehle, A.J. Forty and D. van Rooyen, Editors), held September 11–15, 1967, The Ohio State University, OH, National Association of Corrosion Engineers, Houston, TX, pp. 118–158.

Raicheva S N, 1984. The effect of the surface state on the electrochemical behaviour of copper electrodes. Electrochimica Acta 29, 1067–1073.

Rosborg B, Werme L, 2001. The resistance of pure copper to stress corrosion cracking in repository environments. Presentation at 2001 MRS Spring Meeting, San Francisco, May 2001. (In SKB TR-01-25).

Ryan S R, Clarke C F, Ikeda B M, King F, Litke C D, McKay P, Mitton D B, 1994. An investigation of the long-term corrosion behaviour of selected nuclear fuel waste container materials under possible disposal vault conditions. Atomic Energy of Canada Limited Technical Record, TR-489.

Saario T, Laitinen T, Mäkelä K, Bojinov M, 1999. Literature survey on stress corrosion cracking of Cu in presence of nitrites, ammonia, carbonates and acetates. Posiva Working Report 99–57.

Sato S, Nagata K, 1978. Stress corrosion cracking of phosphorus deoxidised copper. J. Japan Copper and Brass Research Association 17, 202–214.

Sieradzki K, Newman R C, 1985. Brittle behaviour of ductile metals during stress-corrosion cracking. Phi. Mag. A 51, 95–132.

Sieradzki K, Kim J S, 1992. Etch pitting and stress-corrosion cracking of copper. Acta Metallurgical Material 40, 625–635.

Shalaby H M, Al-Kharafi F M, Gouda V K, 1989. A morphological study of pitting corrosion of copper in soft tap water. Corrosion 45, 536–547.

SKB, 1983. Final storage of spent nuclear fuel – KBS-3. Swedish Nuclear Fuel Supply Company Report, KBS-3, Volumes I–IV.

Sosa M, Patel S, Edwards M, 1999. Concentration cells and pitting corrosion of copper. Corrosion 55, 1069–1076.

Sridhar N, Cragnolino G A, 1993. Effects of environment on localized corrosion of copper-based, high-level waste container materials. Corrosion 49, 967–976.

Suzuki Y, Hisamatsu Y, 1981. Stress corrosion cracking of pure copper in dilute ammoniacal solution. Corrosion Science 21, 353–368.

Uchida H, Inoue S, Koyama M, Morii M, Koterazawa K, 1991. Susceptibility to stress corrosion cracking of pure copper in $NaNO_2$ solutions. Society of Material Science Japan 40, 1073–1078.

Werme L, Sellin P, Kjellbert N, 1992. Copper canisters for nuclear high level waste disposal. Corrosion aspects. SKB TR 92-26. Svensk Kärnbränslehantering AB.

Werme L, 1998. Design premises for canister for spent nuclear fuel. SKB TR-98-08. Svensk Kärnbränslehantering AB.

Werme L, 2000. Fabrication and testing of copper canister for long term isolation of spent fuel. In Scientific Basis for Nuclear Waste Management XXIII, (R.W. Smith and D.W. Shoesmith, Editors), Material Research Society Proceedings, Volume 608, Pittsburgh, PA, 77–88.

Yu J, Parkins R N, 1987. Stress corrosion crack propagation in α-brass and copper exposed to sodium nitrite solutions. Corrosion Science 27, 159–182.

Yu J, Parkins R N, Xu Y, Thompson G, Wood G C, 1987. Stress corrosion crack initiation in α-brass exposed to sodium nitrite solutions. Corrosion Science 27, 141–157.

ISSN 1404-0344

CM Digitaltryck AB, Bromma, 2004